IMPACT OF FOUNDATION MODELING ON THE ACCURACY OF RESPONSE HISTORY ANALYSIS OF A TALL BUILDING

Farzad Naeim[1], Salih Tileylioglu[2], Arzhang Alimoradi[1] and Jonathan P. Stewart[2]

[1] John A. Martin & Associates, Inc., Los Angeles, California
[2] Department of Civil & Environmental Engineering, University of California, Los Angeles

Abstract

Soil-structure interaction can affect the response of buildings with subterranean levels by modifying the characteristics of input motions relative to those in the free-field and through the added system compliance associated with relative foundation/free-field translation and rocking. While procedures are available to account for these effects, they are seldom utilized in engineering practice. Our objective is to examine the importance of these effects on the seismic response of a 54 story building with four subterranean levels. We first generate a "most accurate" (MA) model that accounts for kinematic interaction effects on input motions, depth-variable ground motions along basement walls, compliant structural foundation elements, and soil flexibility and damping associated with translational and rocking foundation deformation modes. With reasonable tuning of superstructure damping, the MA model accurately reproduces the observed response to the 1994 Northridge earthquake. We then remove selected components of the MA model one-by-one to test their impact on building response. Factors found to generally have a modest effect on building response above ground level include compliance of structural foundation elements, kinematic interaction effects (on translation or rocking), and depth-variable ground motions applied to the ends of horizontal soil springs/dashpots. Properly accounting for foundation/soil deformations does not significantly affect vibration periods for this tall building (which is expected), but does impact significantly the distribution of inter-story drifts over the height of the structure. Two approximations commonly used in practice are shown to provide poor results: (1) fixing the structure at ground line with input consisting of free-field translation and (2) modeling subterranean soil layers using a series of horizontal springs which are fixed at their far ends and subjected to free-field ground accelerations.

1.0. Introduction

This article is a progress report on an ongoing project investigating the effects of various foundation modeling techniques on the computed response of building structures with embedded foundations. In analyzing the seismic response of a building with a basement, various approaches for modeling the base of the building can be employed. While some of these modeling approaches are very simple, others are complex and require significant effort in modeling the linear or nonlinear soil-structure interaction. What is not clear, however, is whether these more complex and time-consuming approaches actually produce substantially more accurate results.

Currently, over 180 buildings have been instrumented by CSMIP. Out of these, about 35 have subterranean floors and records from at least one earthquake (Naeim, et al. 2005). The four buildings shown in Figure 1 were selected for evaluation in this study. These buildings vary from low-rise stiff buildings to tall and flexible structures, as shown in Table 1. The focus of this article is on the response of Building No. 2 (LA 54 story building) during the 1994 Northridge earthquake.

Our analysis begins with the development of a three-dimensional model, which we call the "most accurate" (MA) model. Each MA model includes soil-foundation-structure interaction in the vertical and horizontal directions, including rocking, with a series of no tension springs and dampers reflecting site soil properties. The MA model of each building includes the embedded portion of the building and its foundations. Seismic demands imposed on the MA model include base translation and rocking (generally from recordings) as well as kinematic loading of basement walls (simulated by displacement histories applied to the ends of horizontal springs attached to basement walls).

Table 1. Buildings and earthquake records considered in this study

No.	*CSMIP ID*	*Name*	*Earthquake records*	*Embedment*	**Site Soil Condition**
1	24652	Los Angeles 6-Story Office	1. 1994 Northridge 2. 2001 Beverly Hills	1 level	Deep Alluvium
2	24629	Los Angeles 54 Story Office	1. 1994 Northridge 2. 1999 Hector Mines	4 levels	Alluvium
3	58503	Richmond 3 Story Gov. Office	1. 1989 Loma Prieta	1 level	Deep Alluvium
4	24322	Sherman Oaks 13 Story Office	1. 1987 Whittier 2. 1994 Northridge	2 levels	Alluvium

Using the aforementioned specification of "seismic demand," the MA model is calibrated to match the response interpreted from the recorded motions. Once the MA model successfully matches the recorded data, we replace components of the specified seismic demand and soil-foundation-structure interaction model (i.e., portions of the MA model that are below ground), one or more at a time, with various simplifications common in practice and assess the errors induced by each simplification on our estimates of various metrics of seismic response.

Many previous studies have been similar to the "MA" component of this work, in that they have developed mathematical models that replicate the recorded response of buildings (e.g., Chajes et al., 1996; Ventura et al., 2003; Kunnath et al., 2004; Liu et al., 2005). The novel aspect of the present work follows the MA model development. Those subsequent models simplify the MA model (without further calibration) so that the degree of error associated with each simplification can be evaluated. The objective is to find the simplest models which produce results of sufficient accuracy for engineering applications.

Following this introduction, we describe in Section 2 the attributes of the LA 54 story building. In Sections 3 and 4 we review a robust SFSI modeling procedure for buildings with subterranean levels and various simplifications to that procedure, respectively. Section 5 describes the challenges we faced with implementing the components of the SFSI model in a conventional structural analysis software package (ETABS). Finally, Sections 6 and 7 present the results of the study and conclusions, respectively.

(a) Building No. 1

(b) Building No. 2

(c) Building No. 3

(d) Building No. 4

Figure 1. Photos and instrumentation sketches for the buildings considered in this study

2.0 Details of the Los Angeles 54 Story Building

2.1. Structural and Foundation Systems

The building is 52 stories tall above ground level with a penthouse and a four-level basement. As shown in Figure 2, the building is roughly rectangular in plan with base dimensions of approximately 212 ft. by 136 ft, tapering inward at the 36th and 46th floors to 196 by 121 ft and 176 by 121 ft, respectively. The vertical load carrying system consists of composite concrete slabs (2.5 inches thick) over a 3 in. steel metal deck with welded metal studs, supported by steel frames. The spans between gravity columns vary from about 10 feet to 47 feet. The lateral load resisting system consists of moment resisting perimeter steel frame (framed tube) with 10 ft. column spacing. There are Virendeel trusses and 48 inch deep transfer girders at the setbacks at the 36th and 46th floors.

The foundation system consists of a reinforced concrete mat that is 9.5 ft thick in load bearing areas and 7 ft thick in intermediate areas. Concrete basement walls surround the subterranean levels.

2.2 Geotechnical Conditions

Geotechnical conditions at the site were characterized by LCA (1981) and are summarized by Stewart and Stewart (1997). The site exploration by LCA generally encountered 65 ft of sands with variable layers of silts and clays overlying siltstone and shale bedrock, which extended to the maximum depth explored of 130 ft. The shear wave velocities shown in Figure 3 are based on in situ downhole measurements by LCA (1981).

2.3 Recorded motions

The building is instrumented with 20 accelerometers (sensors) as shown in Figure 2. Sensors 1 and 2 installed on the top of the mat foundation measure vertical acceleration. The earthquakes recorded at the site are from 1992 Big Bear and Landers, 1994 Northridge, 2001 Hector Mine, and 2008 Chino Hills. The Northridge earthquake produced horizontal ground motions of about 0.14 g at the site whereas horizontal accelerations produced by Big Bear, Landers, Hector Mine and Chino Hills earthquakes were about 0.03 g, 0.04 g, 0.06 g and 0.02g, respectively.. In this article, we focus on the Northridge recordings.

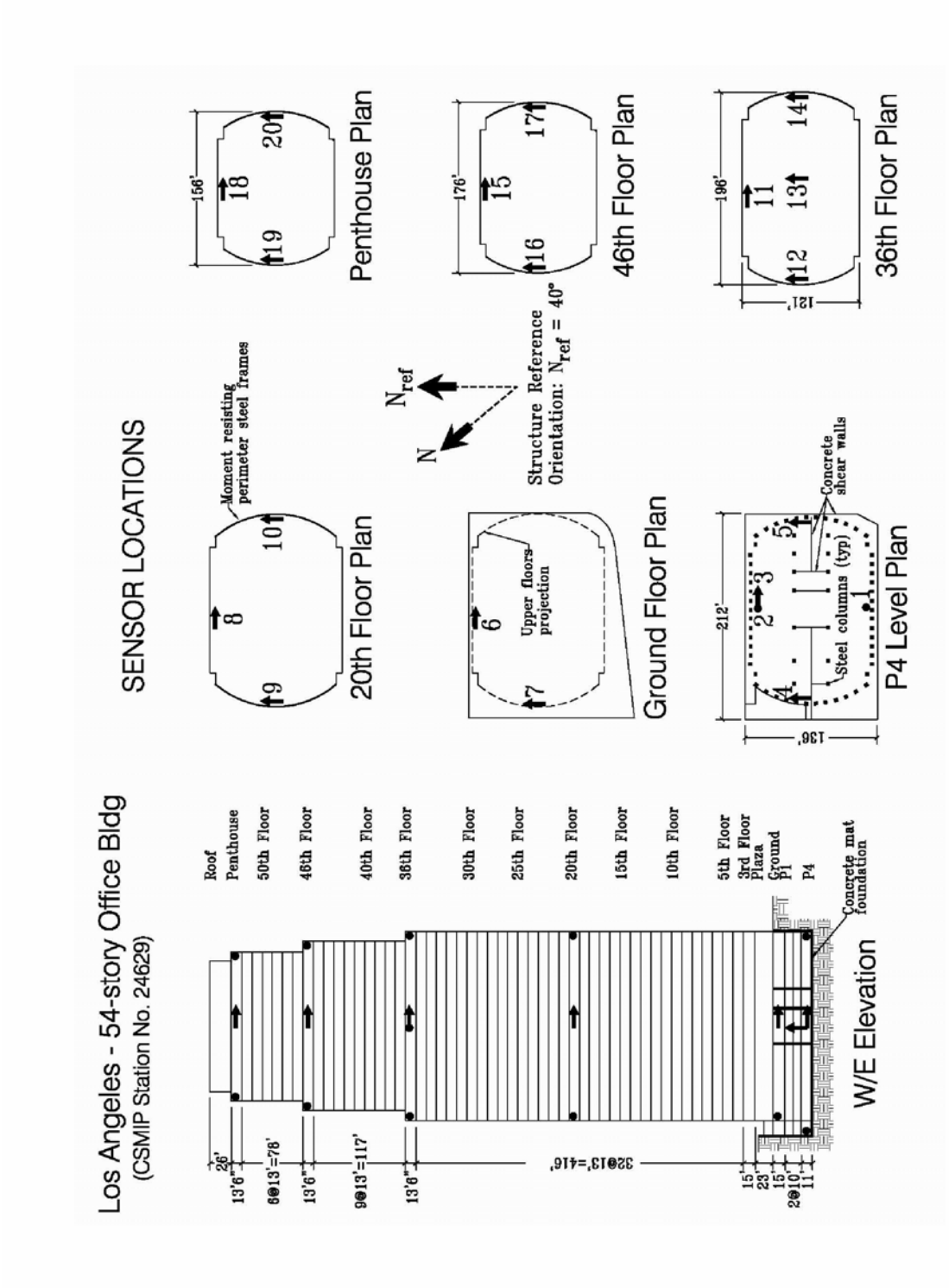

Figure 2. Instrumentation plan of the Los Angeles 54 Story Building

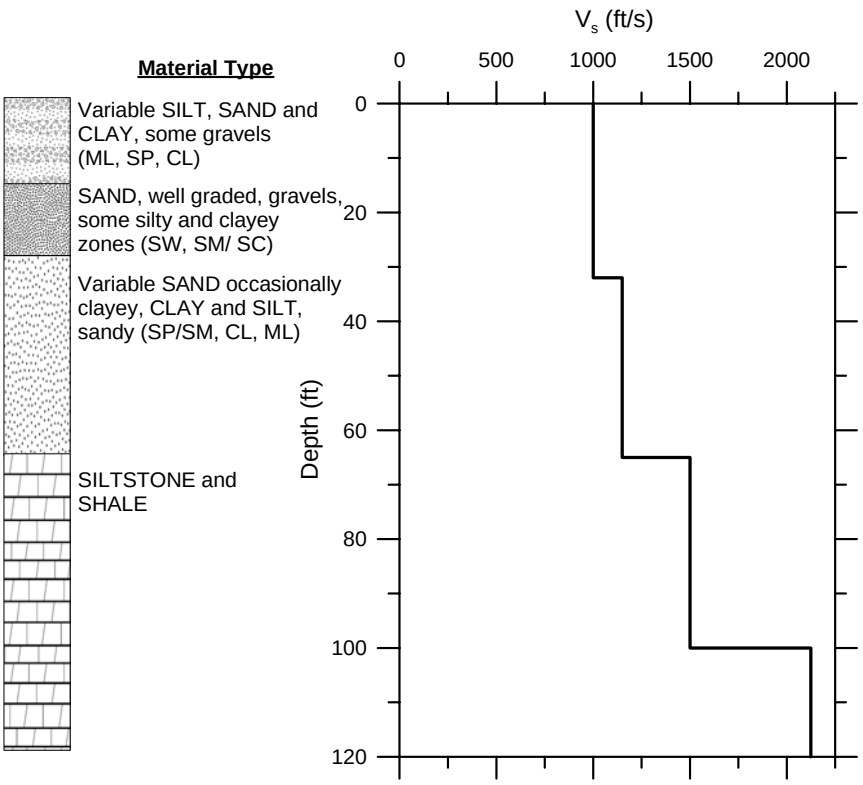

Figure 3. Geotechnical and shear wave velocity profile at LA 54 story building site

3.0 Soil-Foundation-Structure Interaction (SFSI) Modeling Procedures

3.1 General Procedures

SFSI modeling procedures have been recently presented by Stewart and Tileylioglu (2007). The following is extracted from that previous publication.

A schematic illustration of a building with subterranean levels is shown in Figure 4a. The actual soil-foundation-structure system is excited by a wave field that is incoherent both vertically and horizontally and which may include waves arriving at various angles of incidence. These complexities of the ground motions cause foundation motions to deviate from free-field motions (denoted u_g). This complex ground excitation acts on stiff, but non-rigid, foundation walls and the base slab, which in turn interact with a flexible and nonlinear soil medium having a significant potential for energy dissipation. Finally, the structural system is connected to the base slab, and possibly to basement walls as well.

A substructure approach is used to account for these complex SFSI effects, as illustrated in Figures 4b-d. As shown in Figure 4b, the first step in the substructure approach involves evaluating the motion that would be expected to occur on the foundation slab if the superstructure was absent and the foundation had no mass. This motion is termed the *foundation input motion* (FIM), and it accounts for the complexities of the incident wave field and its

interaction with the stiff foundation system. For deeply embedded foundations, the dominant mechanism affecting base slab motions are embedment effects associated with ground motion reductions that occur below the original ground surface. The analysis of the foundation input motion is commonly referred to as a *kinematic interaction* analysis. The foundation input motion consists of horizontal motions denoted u_{FIM} and rotations denoted θ_{FIM}.

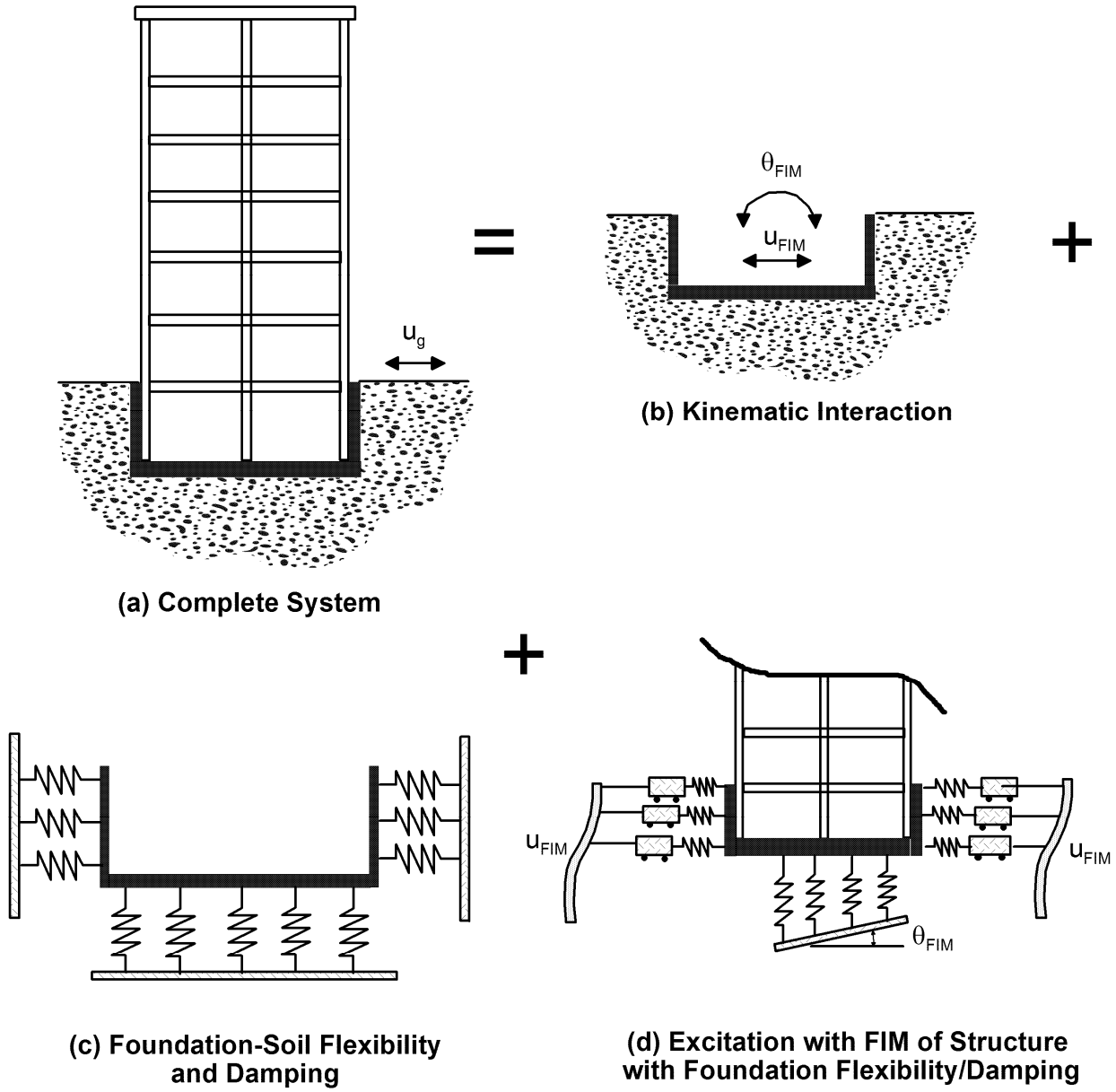

Figure 4. Schematic illustration of the substructure approach to the solution of the soil-foundation-structure interaction problem using distributed foundation springs.

In the second step the stiffness and damping characteristics of the foundation-soil interaction are characterized using a series of distributed springs and dashpots acting around the foundation (illustrated in Figure 4c). Only springs are depicted in Figure 4c for simplicity, but

dashpots are used in parallel to the springs (alternatively, the springs can be visualized as being complex-valued, which accounts for damping).

As shown in Figure 4d, the final step involves placing the superstructure atop the foundation and exciting the system by displacing the ends of the springs using the rocking and translational components of the foundation input motion. Note that differential ground displacements are applied over the height of the basement walls (= depth of embedment) because of the vertical incoherence of ground motion.

3.2 Application to the LA 54 Story Building

There is not a free-field instrument at the LA 54 story building, hence u_g is unknown. What is known is the horizontal translation at the base of the building and the rotation in the short (transverse) direction of the structure (because of the two vertical instruments on the base slab).

The recorded horizontal translation provides a good estimate of u_{FIM}. In reality, the recording is also affected by inertial soil structure interaction effects, which cause the foundation base translation to differ from u_{FIM}. However, those effects are small for buildings such as the LA 54 story building with weak inertial soil-structure interaction effects. Even when they are strong, such effects are narrow-banded at the first mode system frequency (Kim and Stewart, 2003). Hence, we take u_{FIM} as the base mat horizontal recording. Conversely, the base rotation is likely to be dominated by inertial interaction effects, so we do not rely on recordings to estimate this quantity. Instead, it is estimated based on predictions of validated theoretical models (Stewart and Tileylioglu, 2007). Those models allow the estimation of transfer functions that relate free-field motion u_g to the translational and rotational FIMs:

$$\left|H_u\right| = \frac{u_{FIM}}{u_g},\ \left|H_\theta\right| = \frac{\theta_{FIM}}{u_g} \tag{1}$$

where $\left|H_u\right|$ and $\left|H_\theta\right|$ are translational and rotational transfer functions (respectively) that can be evaluated as a function of frequency knowing the soil shear wave velocity and foundation dimension (expressions in Stewart and Tileylioglu, 2007). Figure 5a presents these functions for the LA 54 building site using the aforementioned expressions. Given $\left|H_u\right|$ and $\left|H_\theta\right|$, base rotation can be estimated from u_{FIM} through manipulation of Eq. 1 to yield:

$$\theta_{FIM} = u_{FIM}\frac{\left|H_\theta\right|}{\left|H_u\right|} \tag{2}$$

To summarize, the translational motion applied at the end of the foundation spring attached to the base slab is u_{FIM} (taken from recordings). The vertical motions applied at the end of vertical springs are defined from the product of θ_{FIM} and horizontal distance to the foundation centroid.

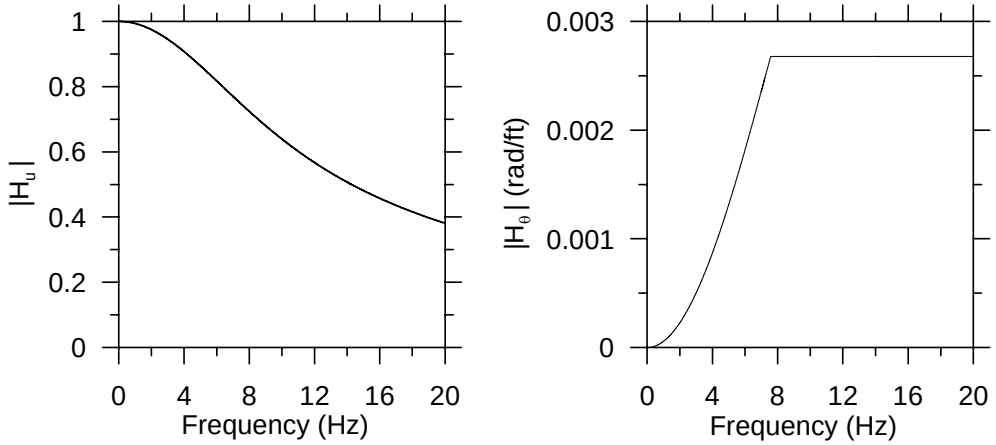

Figure 5a. Theoretical transfer functions between foundation input motions and free-field motion

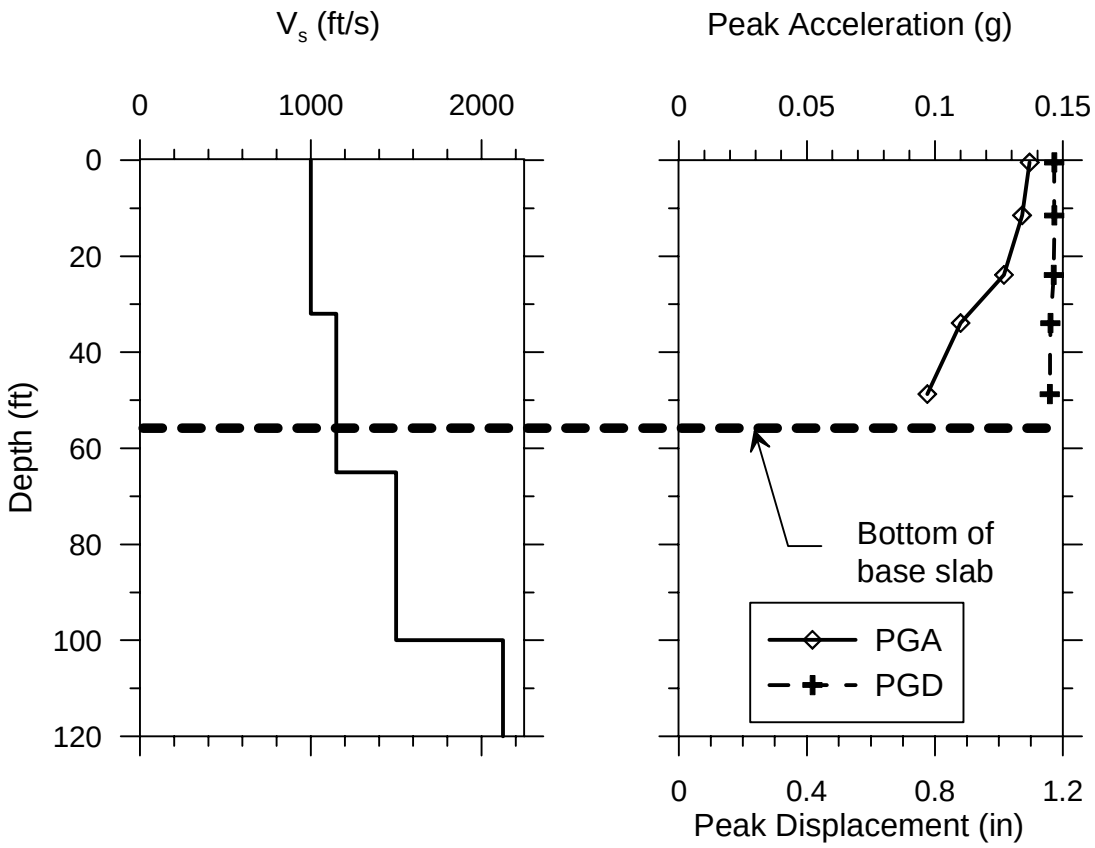

Figure 5b. Variation of peak acceleration with depth at ends of foundation springs, as calculated from ground response analysis.

The remaining issue for ground motion specification is the distribution of translations over the embedment depth, as illustrated in Figure 4d. This is evaluated by performing equivalent-linear ground response analysis with the input consisting of u_{FIM} at the average foundation depth of 46 ft as an outcropping motion. Those analyses were performed with SHAKE04 (Youngs, 2004), which is a modified version of SHAKE91(Idriss and Sun, 1992). We used the velocity profile shown in Figure 3 and nonlinear modulus reduction and damping curves as specified in EPRI (1993), Vucetic and Dobry (1991) and Seed and Idriss (1970). Figure 5b shows that the variation of ground motion over the embedment depth is minor in displacements but is significant in accelerations.

The foundation springs and dashpots are evaluated by first calculating translational (K_x, K_y) and rotational (K_{xx}, K_{yy}) stiffnesses for rectangular rigid foundations (Mylonakis et al., 2002). Dashpot coefficients (C_x, C_y, C_{xx}, C_{yy}) can be similarly evaluated using equations from Mylonakis et al. (2002). Foundation stiffnesses are shown in Figure 6a for the LA 54 story building site. For translation, the portion of the stiffness that can be attributed to the base slab is calculated using surface foundation equations in conjunction with the seismic velocities of materials below the mat. That stiffness is applied as a spring at the elevation of the foundation mat (Figure 4c). The total translational stiffness of the foundation is higher due to embedment, and the difference is applied as horizontal springs distributed along the basement walls. For rotation, vertical springs are distributed along the base of the foundation as shown in Figure 6b. Higher stiffnesses are assigned at the boundaries, but the overall rotational stiffness associated with the vertical springs matches that from the impedance function. This is accomplished by ensuring that the following equalities hold:

$$K_{xx} = \sum_i k_{z,i} \cdot y_i^2 \qquad (3)$$
$$K_{yy} = \sum_i k_{z,i} \cdot x_i^2$$

where K_{xx} and K_{yy} = overall rotational stiffness of foundation (Figure 6a), $k_{z,i}$ = stiffness of vertical spring at location indexed by i, x_i=closest horizontal distance from spring i to the y-centroidal axis of foundation, and y_i=closest horizontal distance from spring i to the x-centroidal axis of foundation. Distances x and y are measured from the centroid as illustrated in Figure 6a. The vertical stiffness values given in Figure 6b satisfy Eq. 3.

Both the horizontal and vertical springs are specified as “compression-only,” meaning that no tension is allowed to develop. This allows a gap to form, although the implementation does not track gap width.

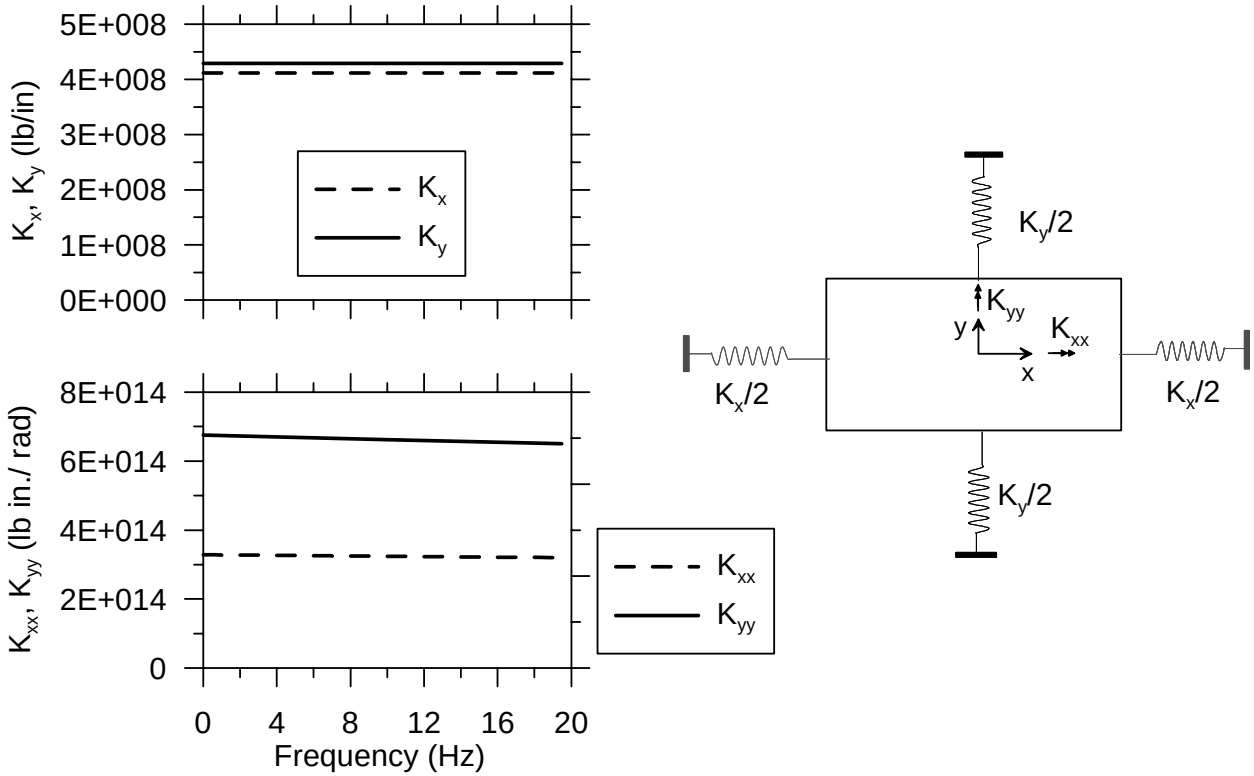

Figure 6a. Foundation impedance functions (stiffness portion) for overall foundation system

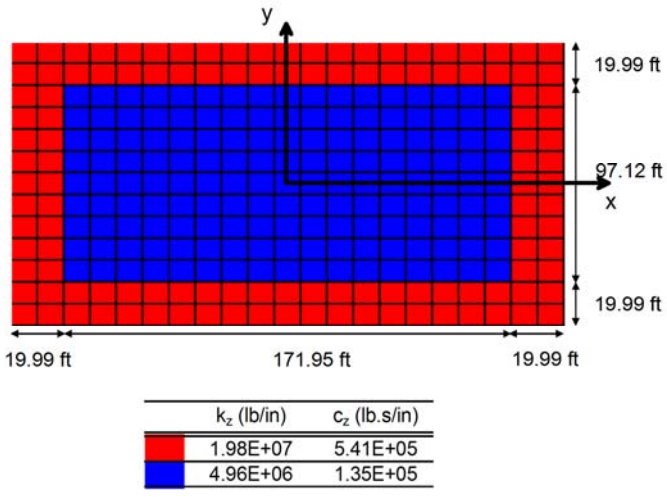

Figure 6b. Distribution of vertical foundation springs and dashpots across base slab

4.0 Simplifications to SFSI Modeling Considered in Present Study

The simplifications to the MA model fall into three categories, as illustrated in detail in Table 2:

Model 1: Replacement of compliant foundation structural elements (i.e., base slab and basement walls) representing actual cracked section properties with rigid elements.

Models 2a-c: Modification of the seismic demand to remove various aspects of the kinematic response and depth-variable ground motions.

Models 3a-d: Modification (or removal) of foundation springs.

Table 2. Summary of the properties of the MA model and the simplified models considered

Model	Compliant Found. Elements	Seismic Demand			Soil Flexibility				
		Kinematic base rocking ($\theta_{FIM}\neq0$)	Depth variant ground motion	Kinematic base translation ($u_{FIM}\neq u_g$)	No-tension springs	H & V springs at base slab	H springs on basement walls	Ignore soil; fix structure at base slab level	Ignore soil; fix structure at ground surface
MA	●	●	●	●	●	●	●		
1		●	●	●	●	●	●		
2a	●		●	●	●	●	●		
2b	●	●		●	●	●	●		
2c	●		●		●	●	●		
3a	●	●	●	●		●	●		
3b	●						●		
3c								●	
3d									●

Details of the specific modifications to the MA model are explained in the following:

1. The embedded portion of the building is assumed to be rigid. The specification of seismic demand is not modified. The objective here is to specifically investigate the effects of compliance in structural elements below ground line.

2. Change the manner in which seismic demand is specified. Three deviations from the MA model are investigated:

    a. Ignore the effect of base rocking in the specification of seismic demand (note that rocking from inertial interaction is still allowed; essentially the ends of the vertical springs on the base slab are not provided with excitations compatible with the rocking that would normally be expected from kinematic interaction).

b. Ignore the effect of kinematic loading of basement walls associated with depth-variable displacement histories applied to the ends of horizontal foundation springs. Essentially, this analysis deviates from the MA model only by fixing the ends of the horizontal springs attached to the basement walls.

c. Neglect kinematic interaction altogether by replacing the recorded motions at the base of the building by equivalent free-field motions (u_g calculated from u_{FIM} using Eq. 1 and Fig 5a; rotation taken as zero).

3. Change the manner in which soil flexibility is modeled. Specifically, we investigate:

a. Allowing springs to develop tension (removal of no-tension interface elements).

b. Neglect entirely soil flexibility at the level of the base slab (i.e., the base slab is fixed vertically and horizontally), and simulate soil flexibility along the basement walls with horizontal springs with ends fixed to match the free-field ground motion. Seismic demand consists only of horizontal motions (equivalent free-field condition) at the base slab level and at the ends of foundation springs. This simulates a condition commonly used in structural design offices.

c. Same as 3(b), except soil flexibility along basement walls is neglected (no soil springs). In this model, the height of the structure is effectively lengthened by the embedment depth and the model is fixed at the level of the base slab. This simulates another condition commonly used in some structural design offices.

d. The below ground portion of the building is ignored and the superstructure is assumed to be fixed at the ground level. Seismic demand consists only of horizontal motions (equivalent free-field condition) applied at ground level. This is the third (and final) condition commonly used in some structural design offices.

5.0 Implementation Issues

Several computing platforms for conducting SFSI analyses were considered. Since our objective was to produce modeling recommendations suitable for adaptation by design offices, we decided to utilize a software system that is most commonly used for dynamic structural analysis of buildings by reputable firms. Therefore, we decided to use ETABS computer program (Computers and Structures, 2008) for this study. Use of more powerful software such as OpenSees (PEER, 2008) may have dramatically reduced the troubles we faced, but would not have produced recommendations that were directly applicable to a design office environment.

Our MA and most other building models are subjected to multiple horizontal and vertical excitations. Horizontal soil springs at various levels and in N-S (y) and E-W (x) directions are excited by distinct input motions at their ends. The vertical springs below the mat foundation are excited by different vertical motions producing rocking of the structure on its base. The current versions of ETABS and SAP2000 can accommodate multiple excitation analysis only if excitations are defined as displacements and not accelerations. Furthermore, if displacement is applied to a node which is part of an integrated system such as a set of interconnected plate

elements representing the mat foundation, only the node excited would move and the other nodes connected to it are not displaced. To get around this issue we devised the modeling scheme presented in Figure 7 where a number of rigid pedestals are introduced at the base. These rigid pedestals are connected to each other at the top by a horizontal rigid plate. The horizontal and vertical ground displacement histories are applied to the bottom end of these rigid pedestals. A set of vertical no-tension springs and dashpots representing vertical soil properties connect this rigid plate to the plate representing the mat foundation above. A series of horizontal no-tension soil springs and dashpots are placed at the edges of the mat foundation and all other subterranean floors as well as the ground floor. The free ends of these springs and dashpots are subjected to the appropriate horizontal ground displacements. Please note that the end displacements imposed on the springs on one side of the building is equal in value and sign to the displacement imposed on the spring at the other side of the building. However, the displacements imposed on different levels are not necessarily the same.

The current version of ETABS (Ver. 9.20) does not offer direct integration as an option. This creates a serious handicap for the SFSI analyses conducted in this study. Nonlinear dynamic analysis in ETABS is conducted via a modified modal analysis technique. Although the nonlinearity in our SFSI analysis is limited to the soil springs (because of the potential for gapping) and therefore could be considered limited in scope, modal analysis poses numerous issues with respect to such analysis. For example, because we are considering the vertical masses and we are modeling the entire gravity system including diaphragms, hundreds of eigenvalues corresponding to individual vibration of floor beams and girders are identified by the program that must be eliminated before the significant structural modes are identified and proper modal damping values are assigned to match recorded motions. Furthermore, extreme care must be taken to ensure that the excited modes include the numerous modes of vibration that should be present to model the behavior of hundreds of soil springs and dampers acting on the basement walls and on the mat foundation. After many trials the only viable solution was to use Ritz vectors instead of eigenvalue analysis in the following manner. First, the vertical masses were ignored and rigid diaphragms were assumed. Eignenvalue analysis was then performed to identify the lateral building modes which had a period of vibration longer than the longest period of vibration of the modes associated with horizontal soil springs. Second, these lateral mode shapes were introduced to the model as a set of Ritz vectors. Third, these Ritz vectors were introduced into the model with vertical masses and floor diaphragms and they were augmented with Ritz vectors representing possible horizontal and vertical displacements of the soil springs and global vertical motion of the building. Fourth, the damping values corresponding to various Ritz vectors were adjusted to match the recorded displacements at the location of sensors.

This modeling technique was successfully used to match recorded displacements throughout the building. However, the accelerations and forces reported by ETABS, particularly at the subterranean levels, were not reliable. As shown in Figure 8, ETABS routinely reported huge acceleration spikes at the first time-step of response history analysis, which was clearly non-physical. This spike is attributed to solution scheme convergence failure. Although this spike could be eliminated by ignoring the results reported for the first time-step of analysis, additional smaller spikes were usually present during the first several seconds of response that we also believe to be non-physical.

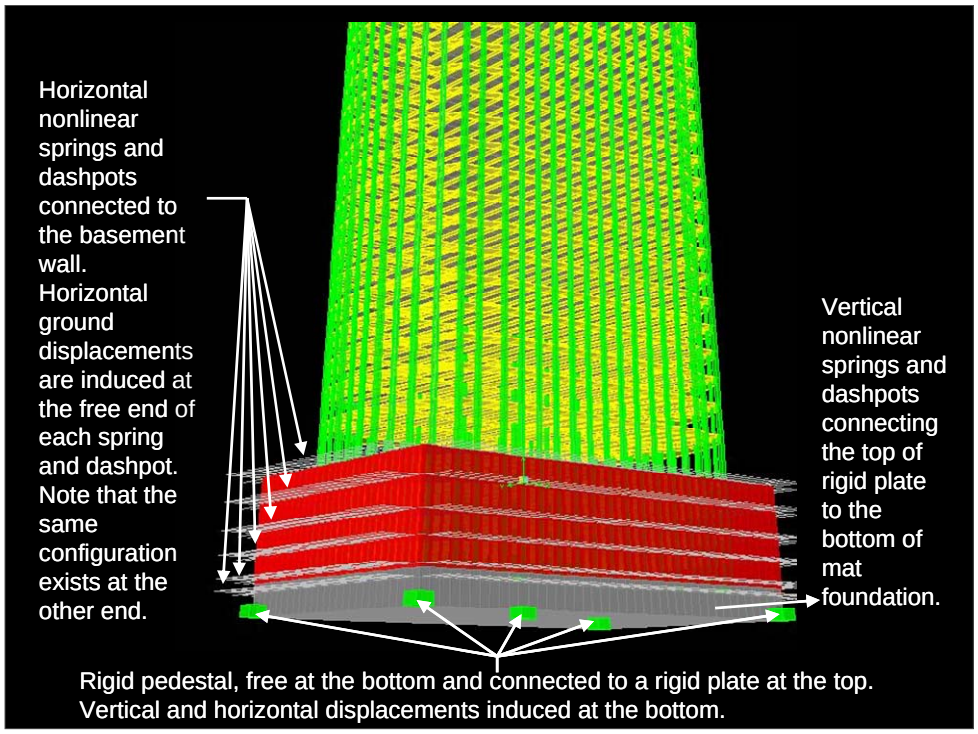

Figure 7. Soil-foundation-structure interaction modeling technique

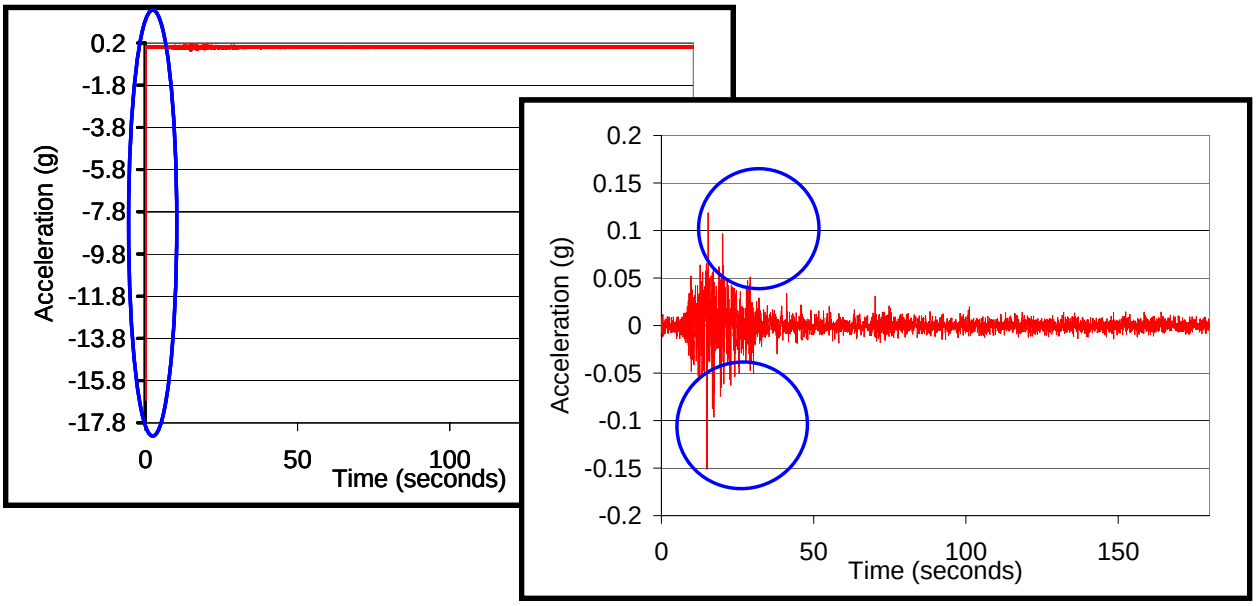

Figure 8. Issues related with computed accelerations obtained from the ETABS model. For models excited with base displacements as shown in Figure 7, ETABS reports an erroneous and huge acceleration spike at the first time step of response-history analysis (see trace to the left). If the spike at the first time step is removed, the trace shown on the right is obtained which still contains smaller spikes which in our opinion are not real and are caused by solution instability.

5.0 Results

6.1 Results for the MA Model

The best match of MA model to recordings was obtained with all modal damping values set to 1.0% of critical except for modes 1 and 4 where the damping values were set to 1.8%. The same damping values were used for all approximations. A summary of 50 Ritz vectors provided a level of accuracy that did not improve by inclusion of more vectors (up to 300 Ritz vectors were utilized to see if there is any significant difference in the results). A summary of the first five periods associated with Ritz vectors for various models is presented in Table 3. As indicated by Table 4 all five computed periods are very close to those identified from recorded data using the CSMIP-3DV software (Naeim, et al. 2005; 2006).

Table 3. Summary of periods associated with the first five Ritz vectors for various models.

Model	Reported vibration periods for first five Ritz vectors (sec.)				
	1	2	3	4	5
MA*	6.06	5.18	2.76	1.92	1.81
1	6.03	5.15	2.75	1.91	1.81
2A	6.06	5.18	2.76	1.92	1.81
2B	6.06	5.18	2.76	1.92	1.81
2C	6.06	5.18	2.76	1.92	1.81
3A	6.04	5.18	2.78	1.92	1.82
3B	5.79	4.99	2.76	1.92	1.82
3C	5.79	4.99	2.76	1.92	1.82
3D	5.63	4.90	2.74	1.89	1.80

Table 4. Comparison of MA model periods and those obtained from system identification

Direction	Identified Periods (sec.)		MA Model Periods (sec.)	
	Mode 1	Mode 2	Mode 1	Mode 2
E-W	6.07	1.95	6.06	1.92
N-S	5.12	1.86	5.18	1.81
Torsional	2.78		2.76	

Displacement histories obtained from the calibrated MA model are compared to recordings in Figure 9. Excellent agreement between recorded and computed vertical and horizontal displacements at the P-4 level (above the mat) may be observed in Figures 9a to 9d. The match in both horizontal directions at the ground level is also virtually perfect (Figures 9e and 9f). Elsewhere over the height of the building the quality of the match is generally better in the E-W direction than in the N-S direction. However, the matching of both maximum amplitudes and phasing are very good in both directions.

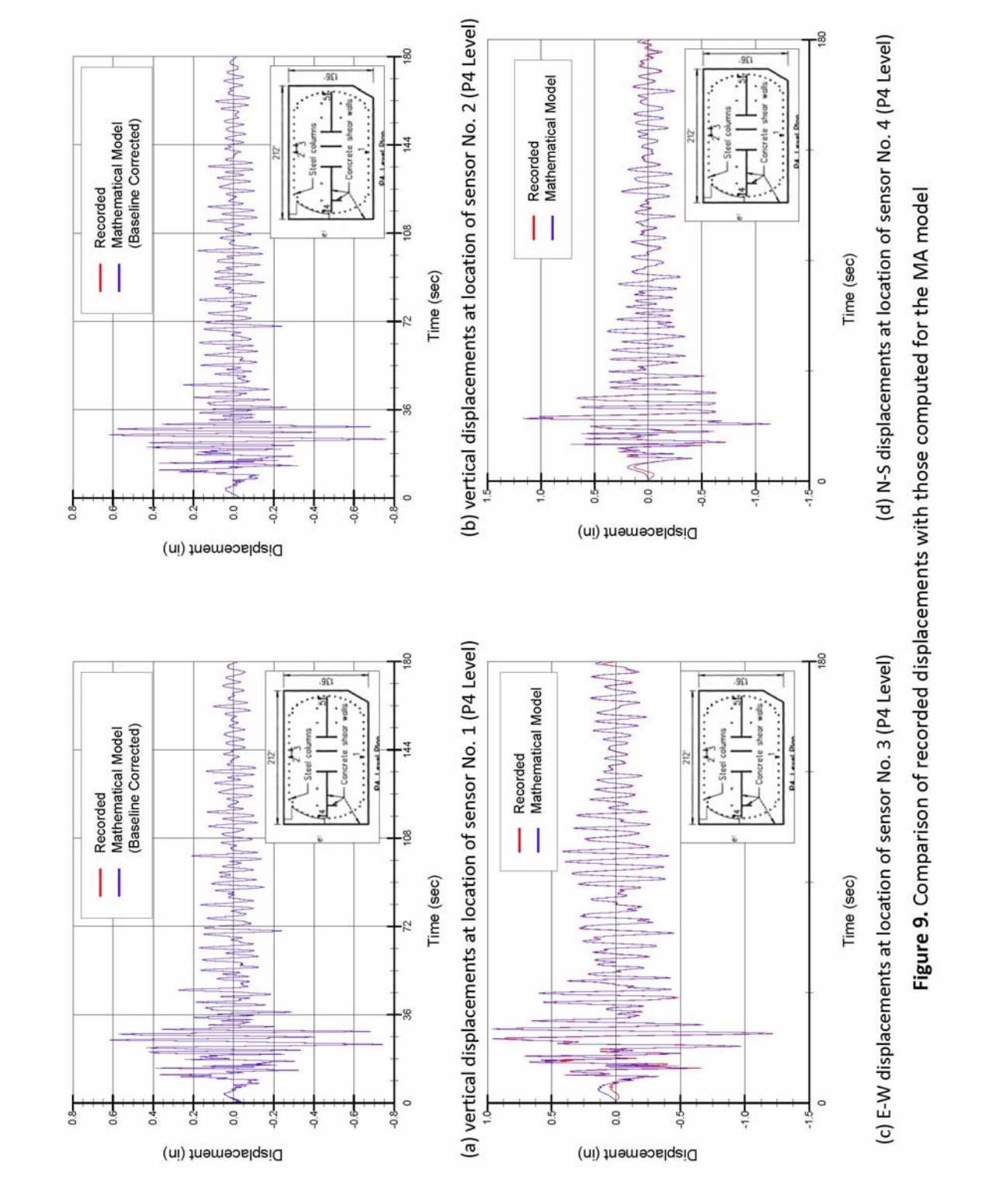

Figure 9. Comparison of recorded displacements with those computed for the MA model

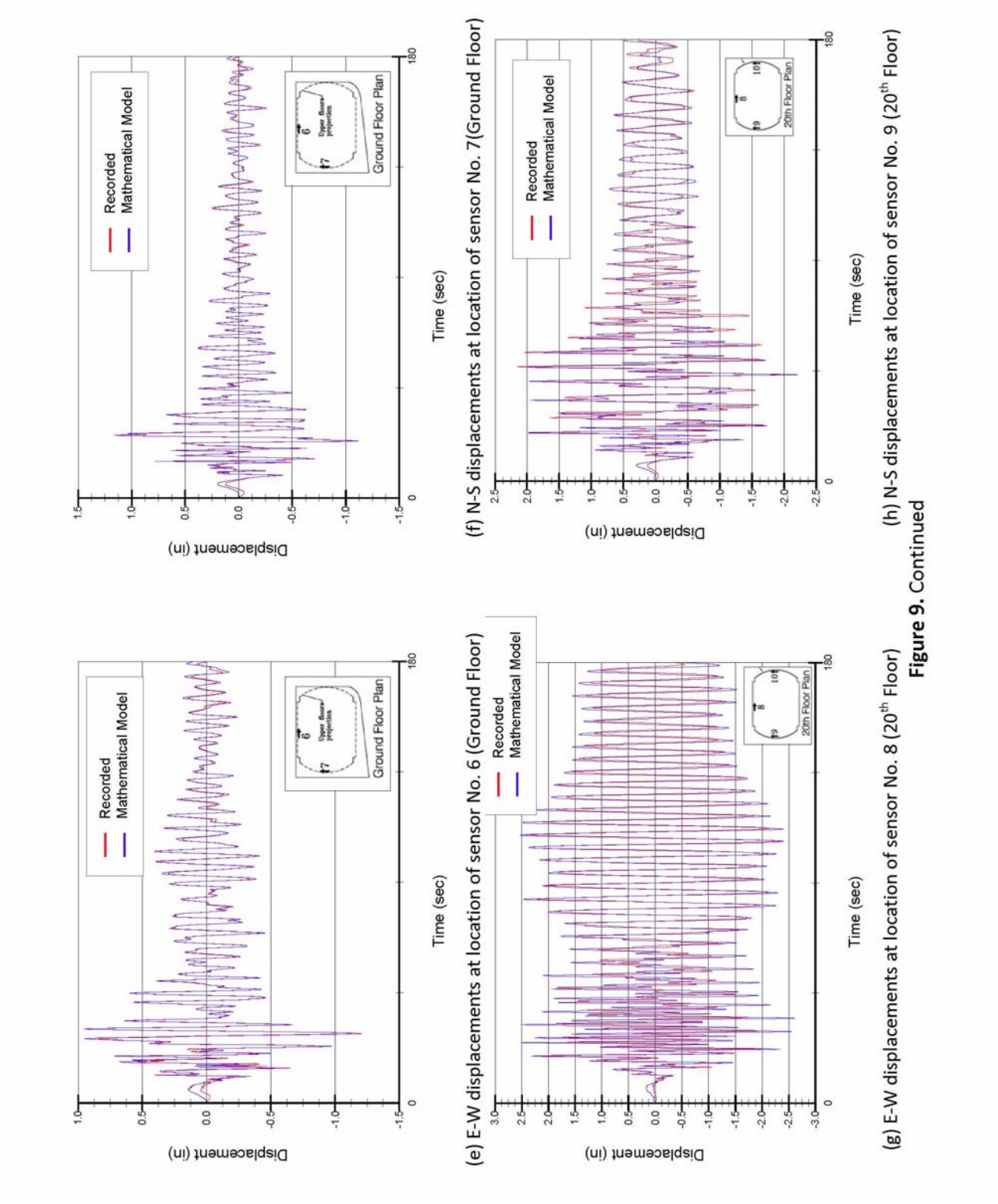

Figure 9. Continued

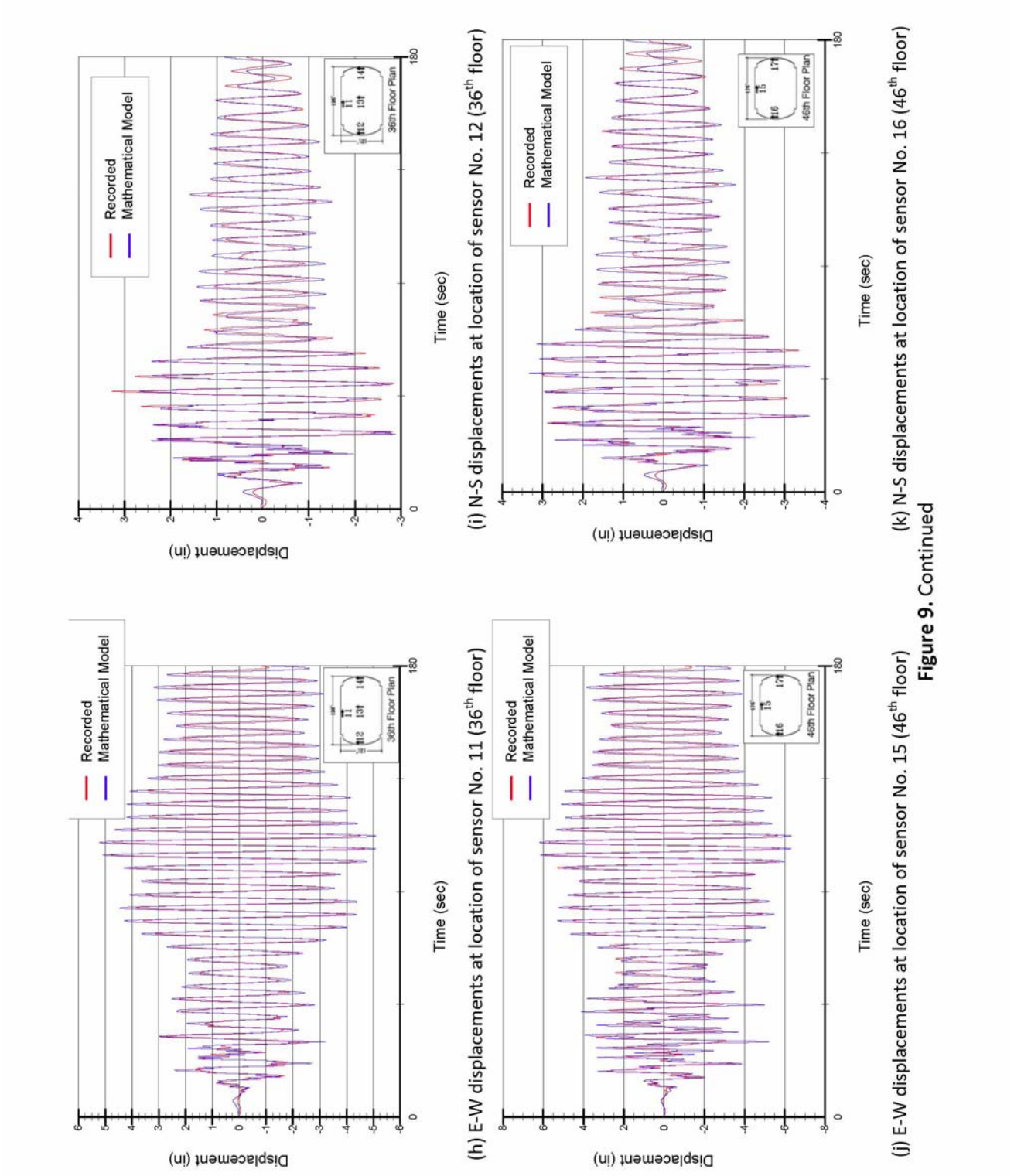

(h) E-W displacements at location of sensor No. 11 (36th floor)

(i) N-S displacements at location of sensor No. 12 (36th floor)

(j) E-W displacements at location of sensor No. 15 (46th floor)

(k) N-S displacements at location of sensor No. 16 (46th floor)

Figure 9. Continued

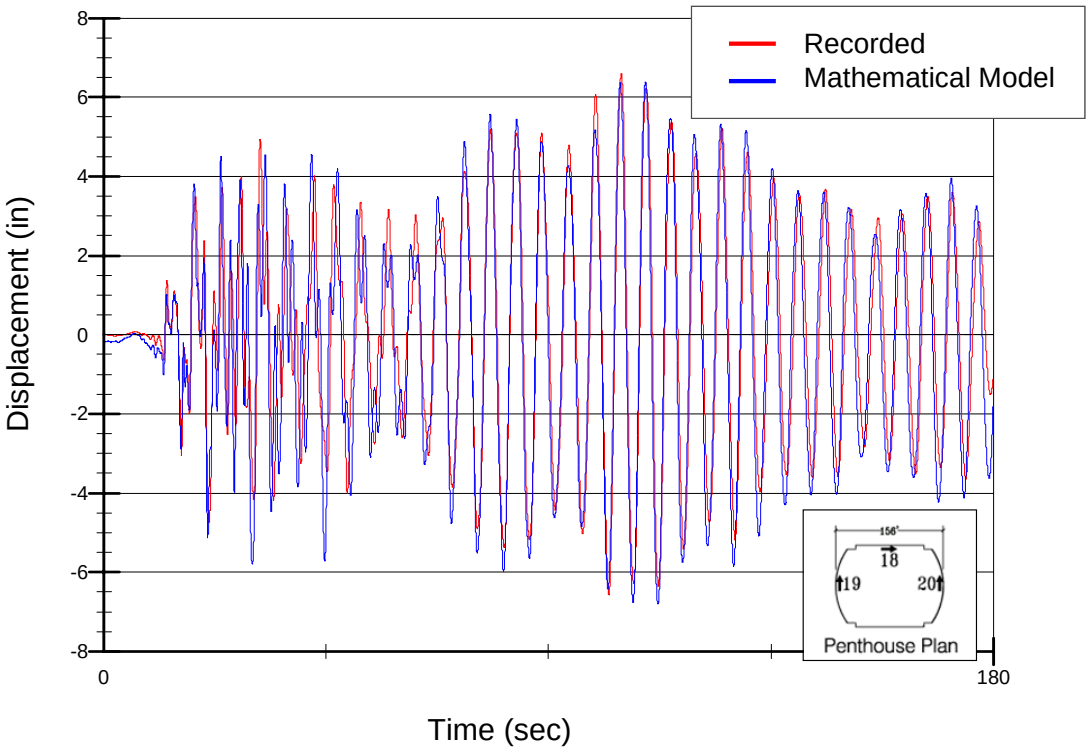

(l) E-W displacements at location of sensor No. 18 (Penthouse)

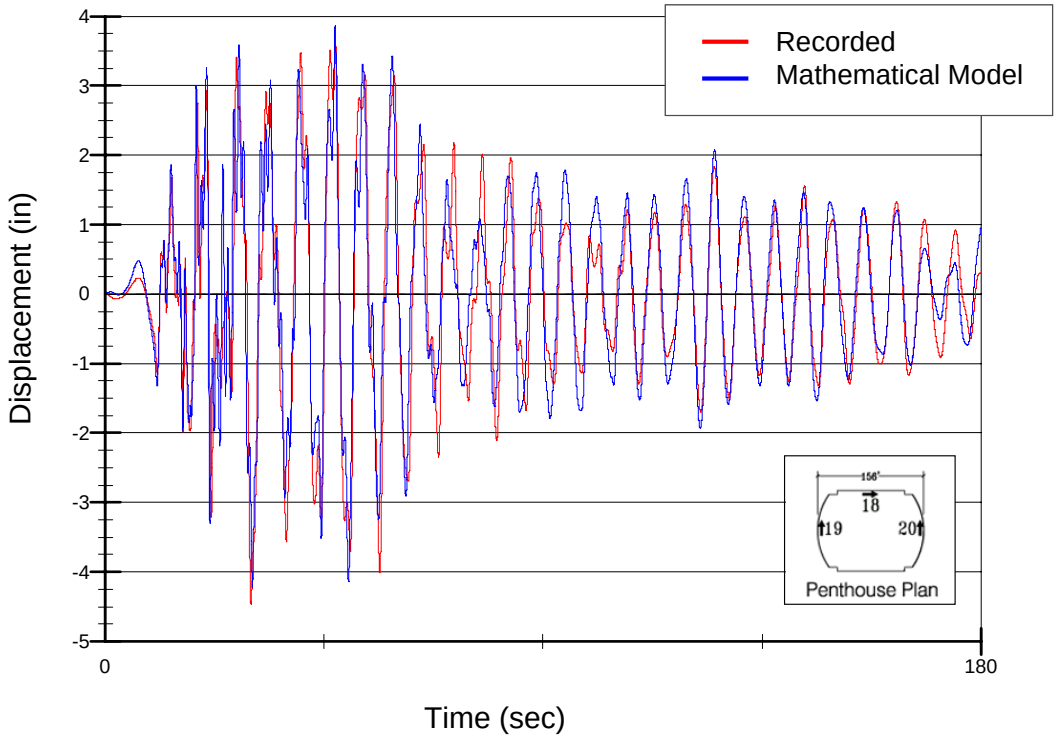

(m) N-S displacements at location of sensor No. 19 (Penthouse)

Figure 9. Continued

6.2 Results for Selected Approximations

Our analyses of the models that are simplified relative to MA are presented relative to the MA results instead of the recordings. This allows for a direct comparison of impact of changes in model attribute.

Allowing tension in the soil with no other changes (Model 3A) does not affect the results by much. Table 3 shows that the building vibration periods are very slightly affected and Figure 10 shows the errors induced in displacement history response throughout the height are negligible (e.g., less than 4% at roof level). As illustrated in Figure 11, error in maximum story drift ratios for floors above ground level are less than 10% and 5% in the E-W and N-S directions, respectively. The error in the maximum interstory drift ratios for subterranean floors are significantly larger at about 32% in the E-W direction and 46% in the N-S direction.

Ignoring the subterranean levels by assuming a rigid base at ground level (Model 3D) significantly alters the vibration periods of the building (see Table 3). As a result, many of the displacement history responses are out of phase with those of obtained for the MA model (see Figures 12b to 12d). The roof peak displacement in the E-W direction for the MA and 3D models while having similar amplitude occurs at very different times during the response (Figure 12c). The error in peak roof displacement is less than 20% (Figures 13a and 13b). Interestingly, the distribution of interstory drifts over the height of the structure is also significantly affected, with drifts increasing at lower levels and decreasing at higher levels of the building for Model 3D relative to MA.

Fixing the far ends of horizontal soil springs, and subjecting these fixed ends to free-field ground accelerations (Model 3B) is one of the two common methods used by engineering offices to bound the SFSI problem. As shown in Table 3, this approximation also significantly affects the dynamic characteristics of the model by shortening its period because the fixed-end springs provide more resistance to the below-ground structure. As shown in Figure 14a-b,the ground level displacements reported by this approximation are negligible compared to those reported by the MA model. Note that in this model the ground accelerations are used as input and ETABS does not calculate the displacements at the fixed ends of the horizontal springs. Therefore, the displacements reported at the ground line consist only of the in-plane displacements of the ground floor diaphragm which are very small. Figures 14c-d show that the displacement histories at roof level are very different from those obtained from MA model. Note that the peak roof displacement in the E-W direction happens to be close to that twice that of the MA model. This is reflected in the maximum displacement and drift charts presented in Figure 15 where the results in the E-W direction look deceptively close to that of MA model while the results in the N-S direction vary sharply from those obtained from the MA model.

Ignoring the embedment effect by running the structure down to the foundation level and ignoring the horizontal stiffness of the surrounding soil is another common assumption that is used in design offices to bound the SFSI problem (Model 3C). Many engineers will be surprised to see that the 3C model is stiffer and has a shorter fundamental period than the MA model (Table 3). As shown in Figure 16, the displacement time histories at the ground floor for the 3C and MA model are virtually identical (Figure 16)). The error in maximum roof displacement is small at less than 5% and 10% in E-W and N-S directions. Figure 17 shows that as with Model

3D, Model 3C story drift ratios increase relative to MA at lower levels of the building, although this effect is principally in the E-W direction.

If we retain all MA model characteristics but assume foundation structural elements (i.e, mat and basement walls) to be rigid (Model **1**), building periods are practically unaffected, as shown in Table 3. Figures 18a-b show that the displacement histories at the ground floor for the **1** and MA model are virtually identical. The frequency match with the MA model results for the displacement histories for are good throughout the height of the building. However, Model **1** overestimates the displacements of the upper portions of the building in the E-W direction in the first one-third of the response duration where the peak displacement in this direction occurs (Figure 18c) resulting in an overestimation of the maximum roof displacement in this direction by about 25% (Figure 19a). In the N-S direction, the reverse occurs. That is, the displacement amplitudes in the early part of the response where peak displacement occurs is very close to those obtained from the MA model but in the later part of the response Model **1** underestimates the amplitude of displacements (Figure 18d). As a result, the maximum story displacements in the N-S direction are much closer to the values reported by the MA model. The maximum error for displacements in this direction is less than 8%. The maximum error in interstory drifts in the E-W direction occurs at the 22nd floor and is about 28%. The maximum interstory drift errors at above ground floors in the N-S direction are significantly smaller at less than 5%. However, the same error in the subterranean levels in the N-S direction is significantly larger in the N-S direction compared to the E-W direction (65% compared to 20%).

Elimination of kinematic base rocking with no other changes (Model 2A) has negligible effect on the vibration periods of the building (Table 3). Moreover, as shown in Figure 20, the maximum displacements and interstory drifts throughout the height of the building, with the exception of subterranean drifts, are almost identical.

Eliminating kinematic loading from relative soil displacements adjacent to basement walls (Model 2B) virtually affects nothing as the displacement and inter-story drift histories and maximum values are nearly identical to those obtained from the MA model (Figure 21).

Finally, ignoring kinematic interaction effects on the base horizontal motion (Model 2C) produces results which are virtually identical to the MA model at all floor above the ground level (Figure 22). However, use of Model 2C results in significant underestimating of maximum interstory drifts in the subterranean levels (Figures 22c and 22d).

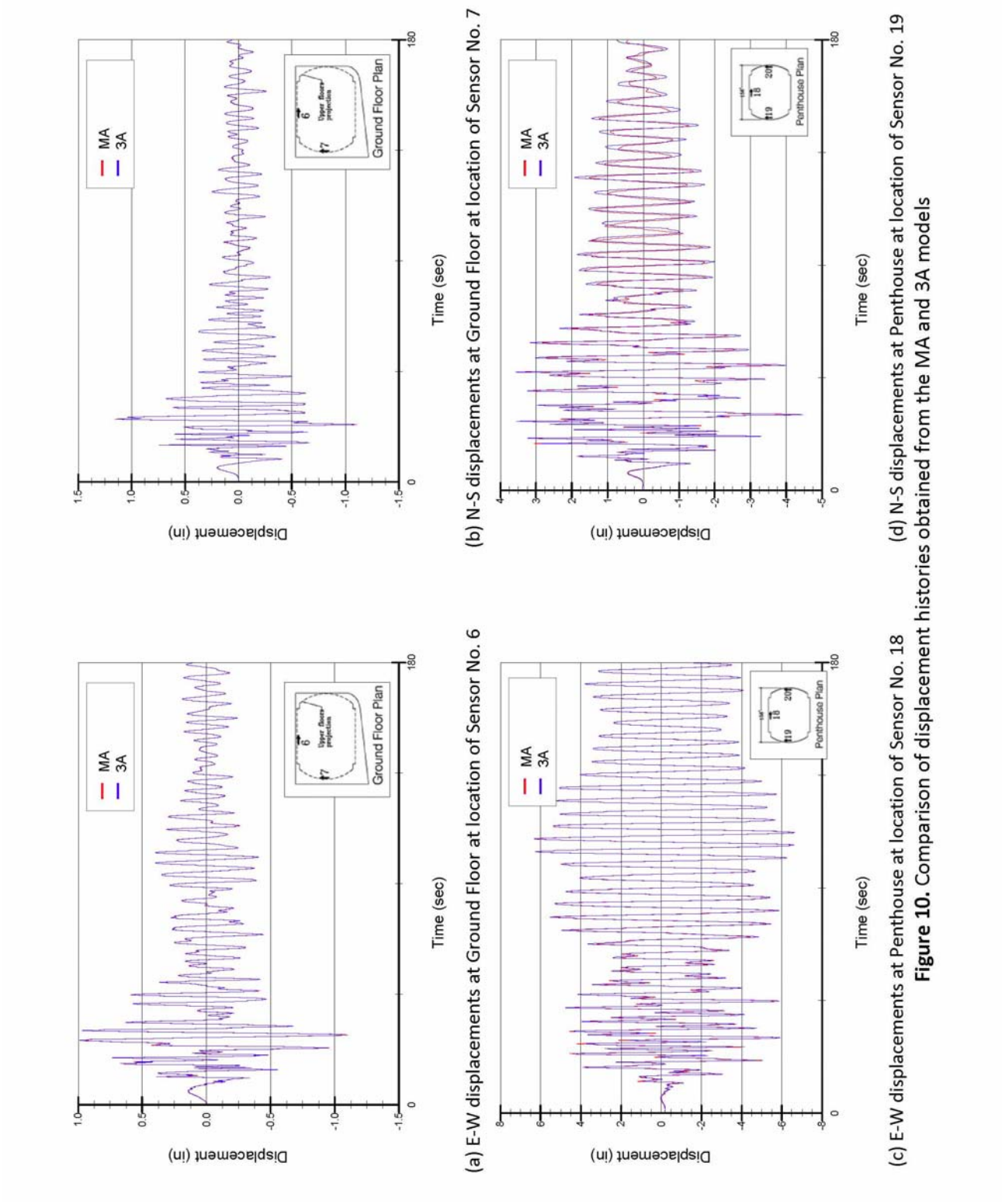

Figure 10. Comparison of displacement histories obtained from the MA and 3A models

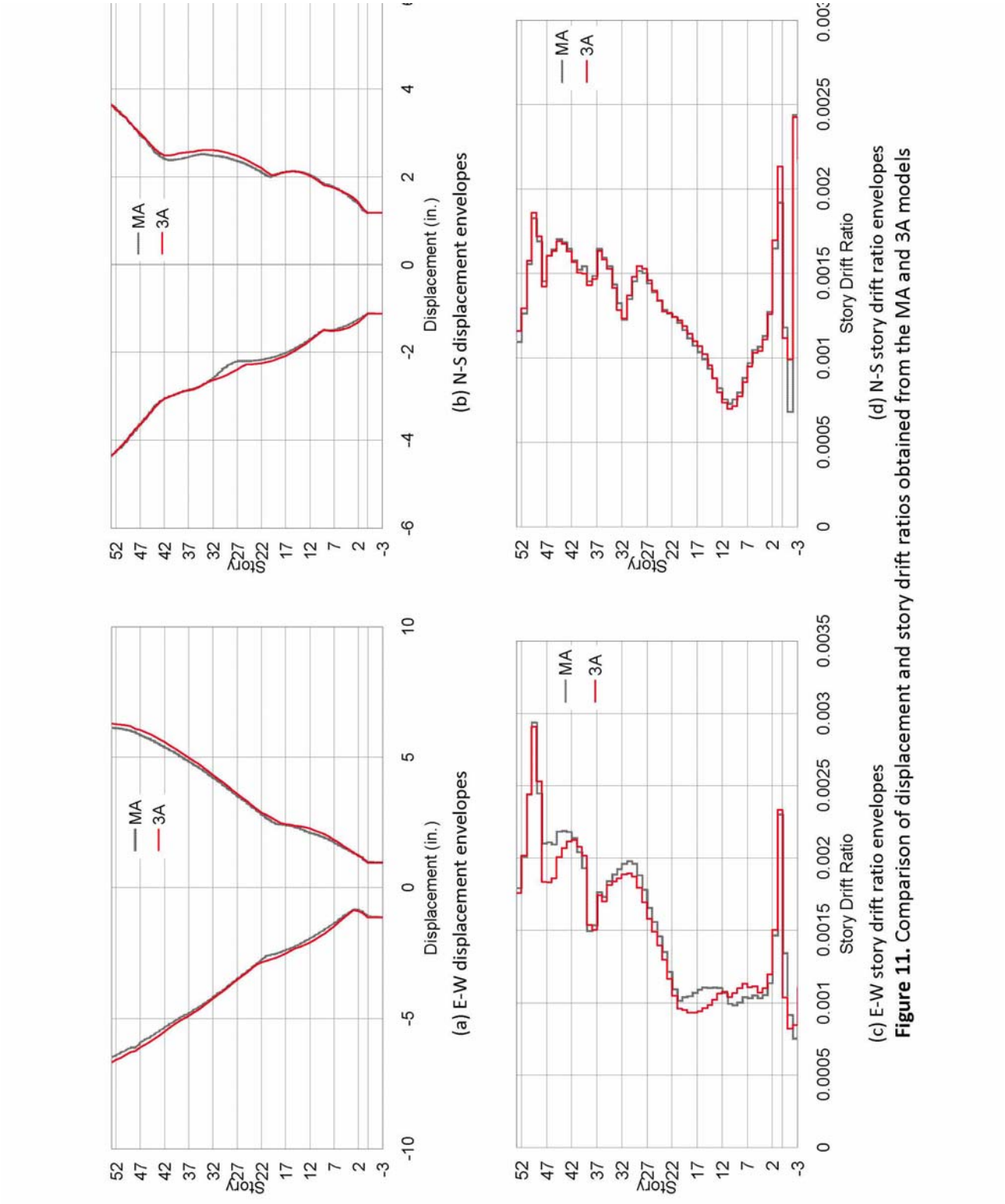

Figure 11. Comparison of displacement and story drift ratios obtained from the MA and 3A models

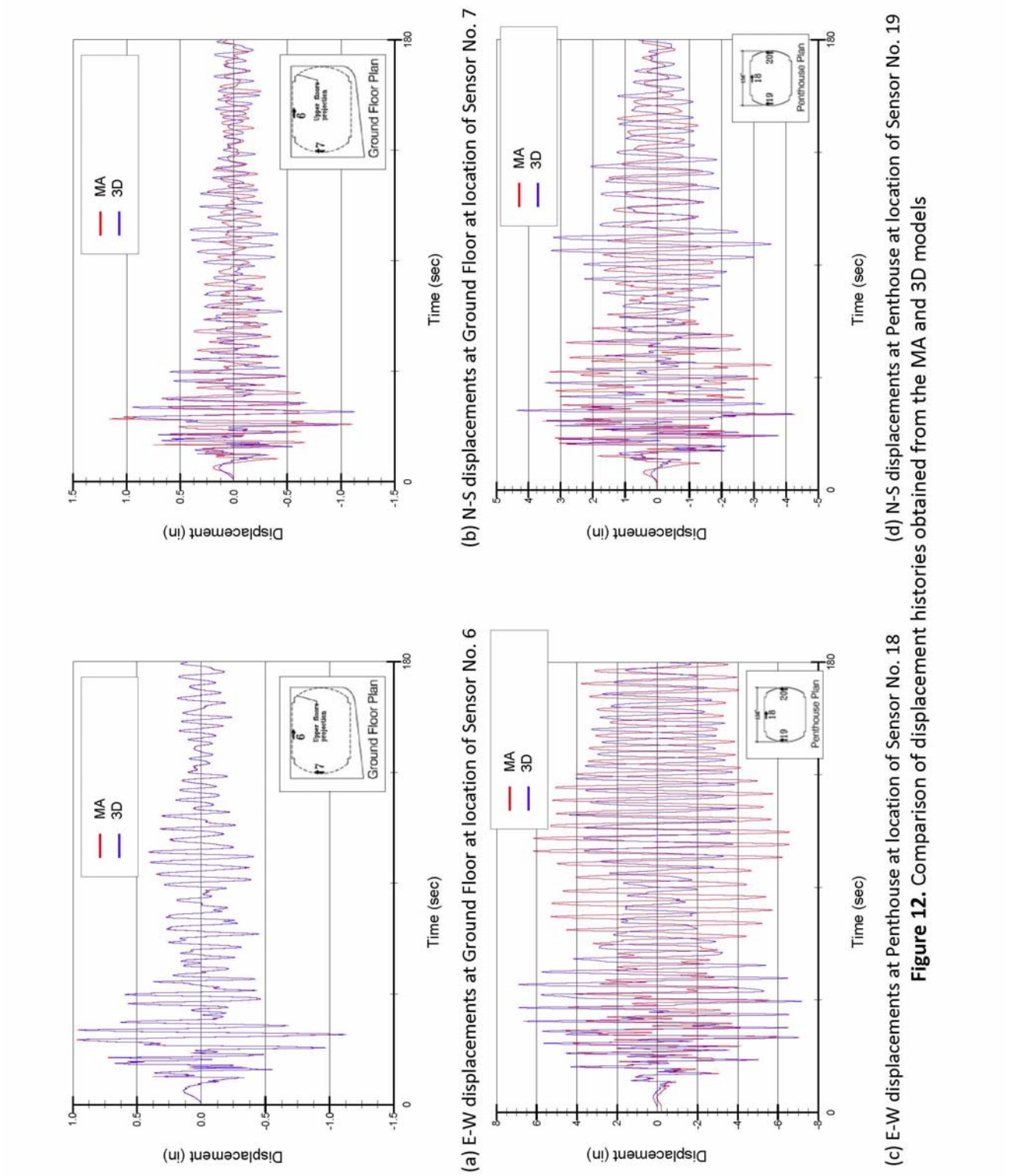

Figure 12. Comparison of displacement histories obtained from the MA and 3D models

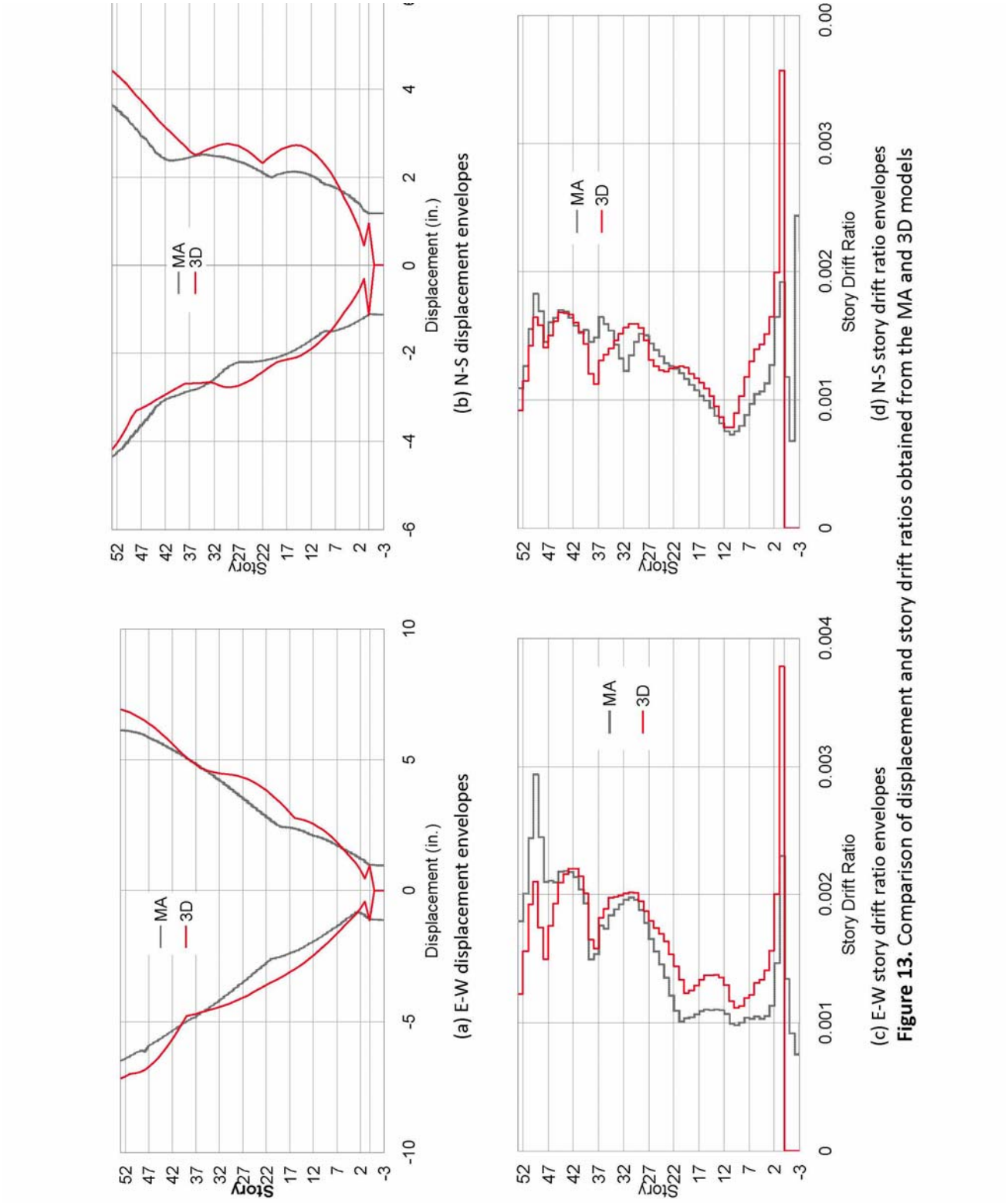

Figure 13. Comparison of displacement and story drift ratios obtained from the MA and 3D models

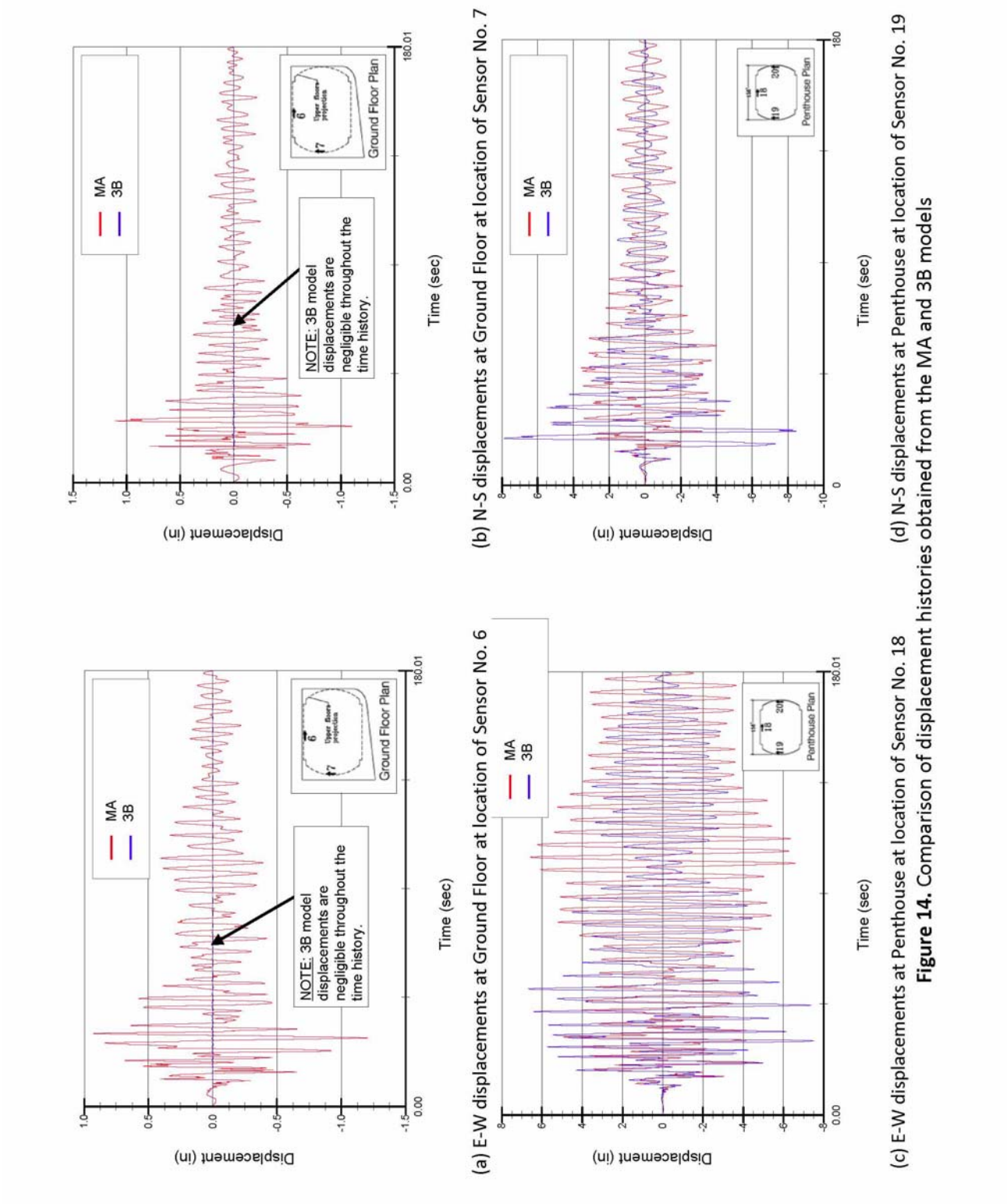

Figure 14. Comparison of displacement histories obtained from the MA and 3B models

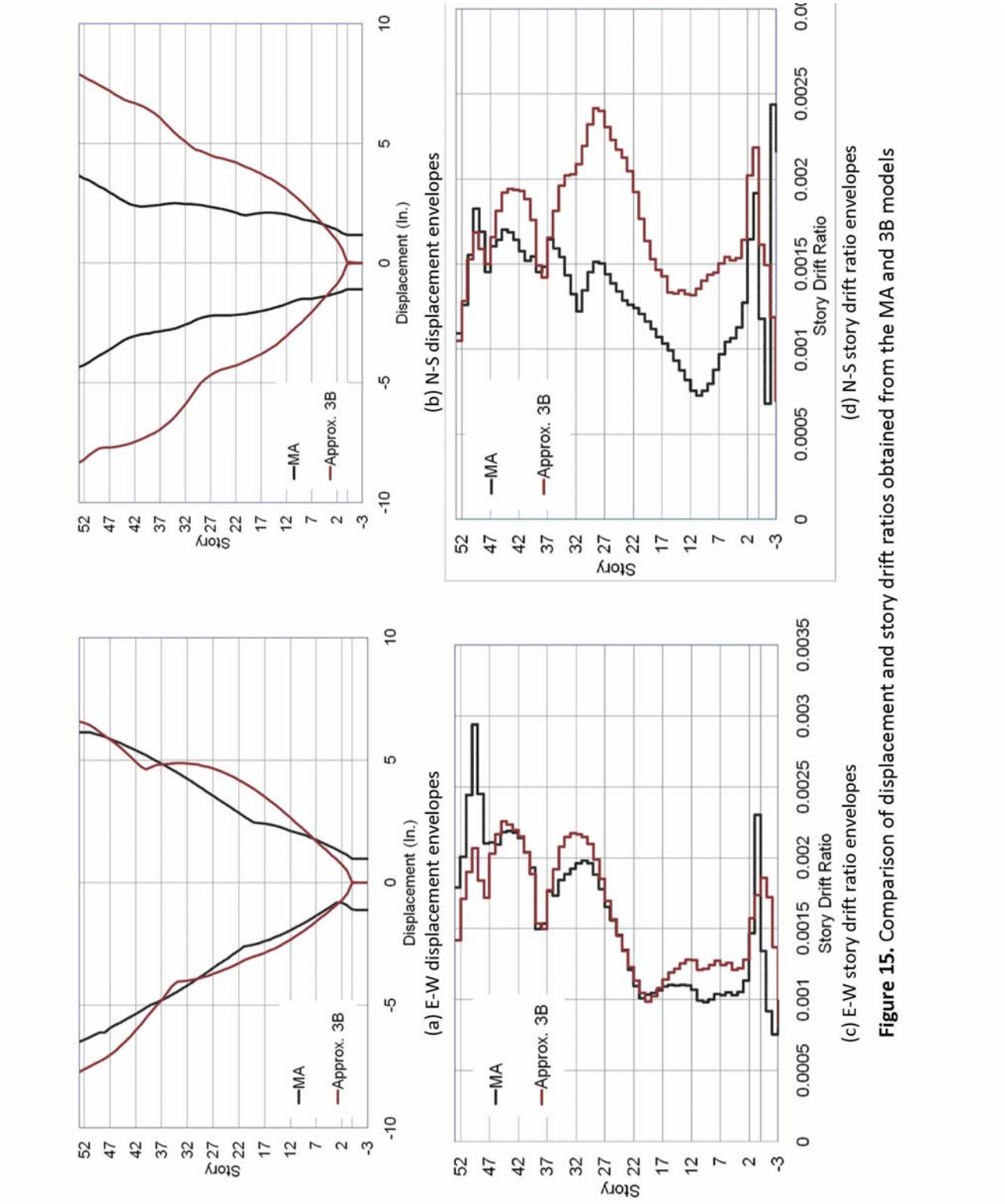

Figure 15. Comparison of displacement and story drift ratios obtained from the MA and 3B models

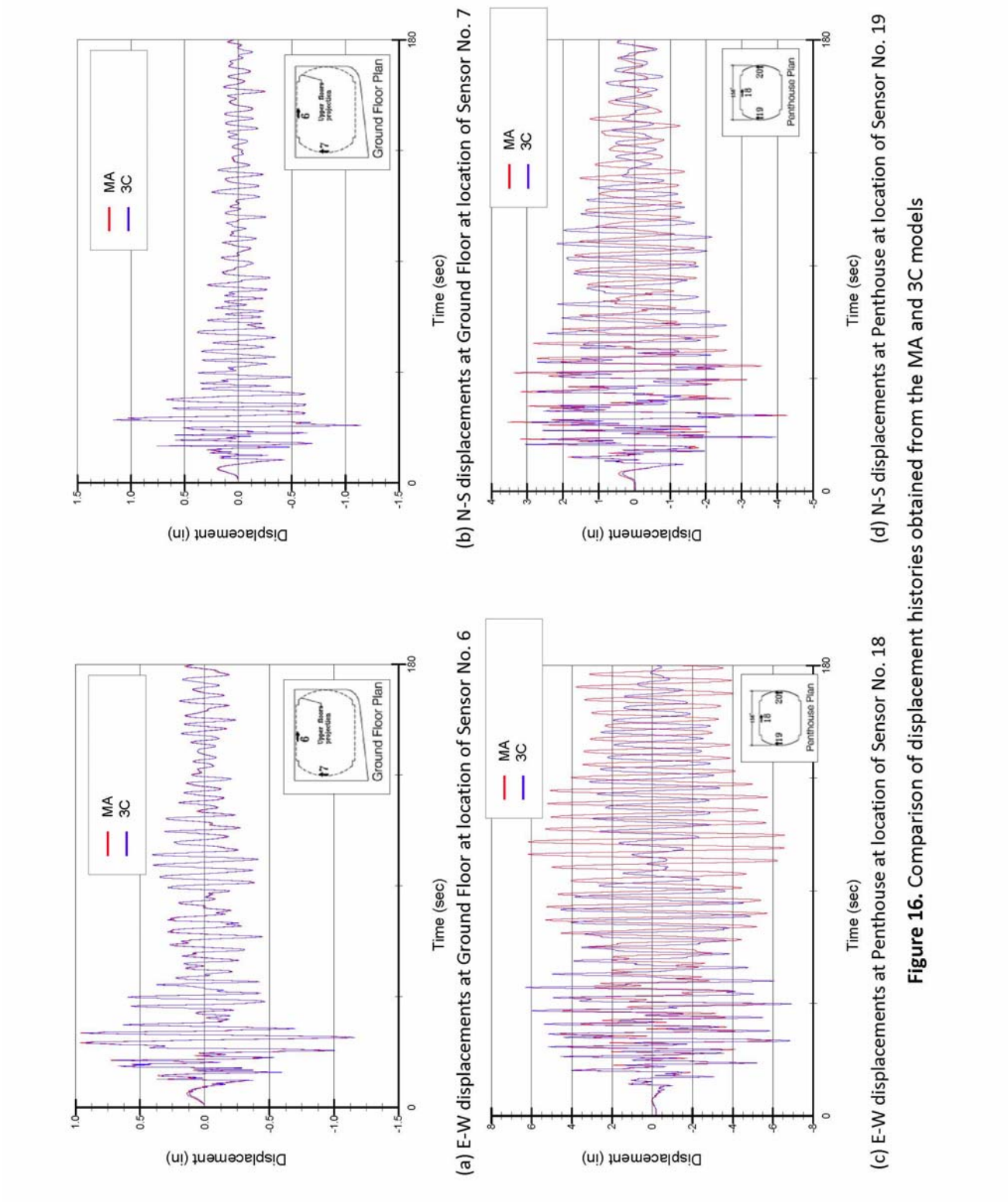

Figure 16. Comparison of displacement histories obtained from the MA and 3C models

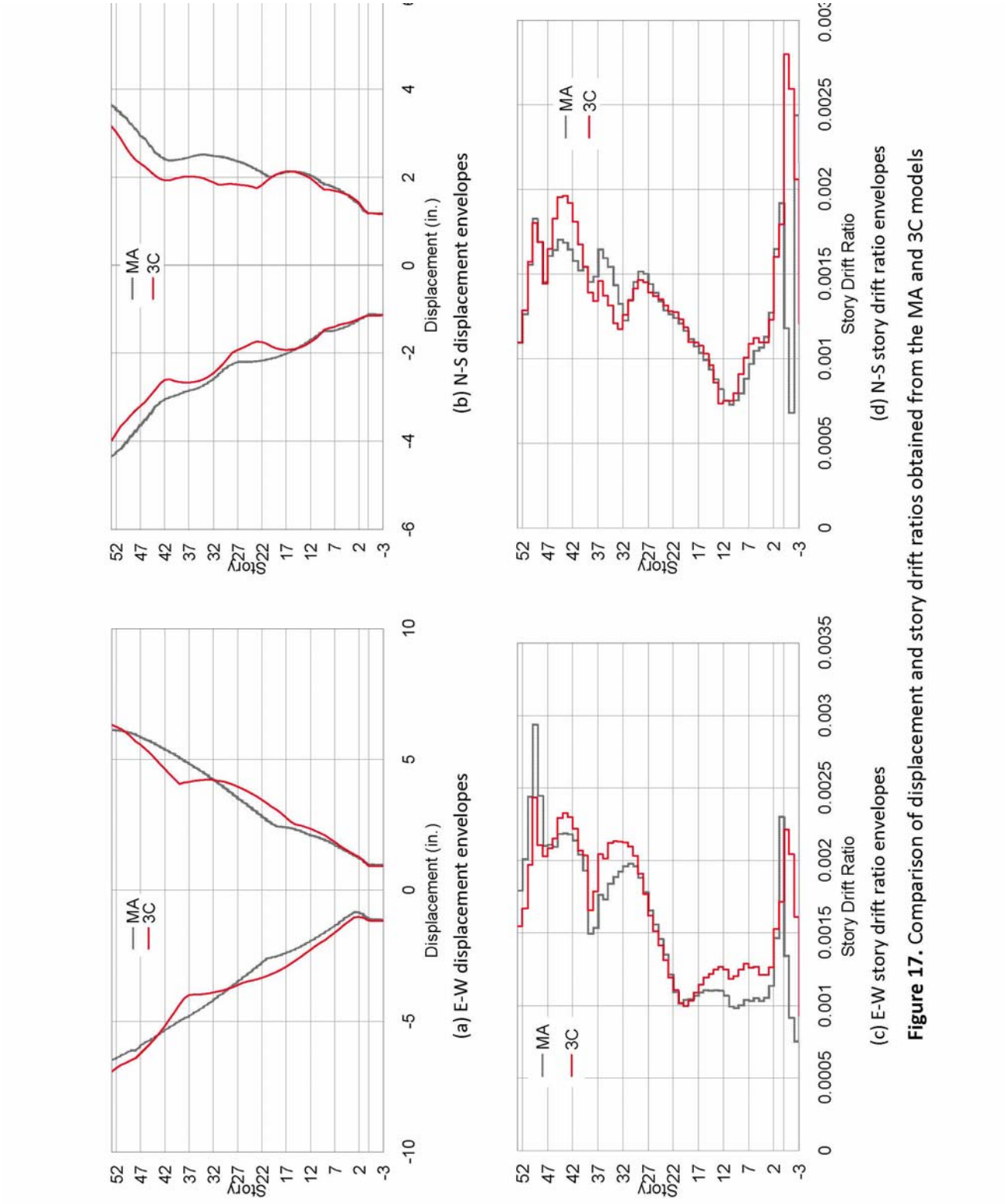

Figure 17. Comparison of displacement and story drift ratios obtained from the MA and 3C models

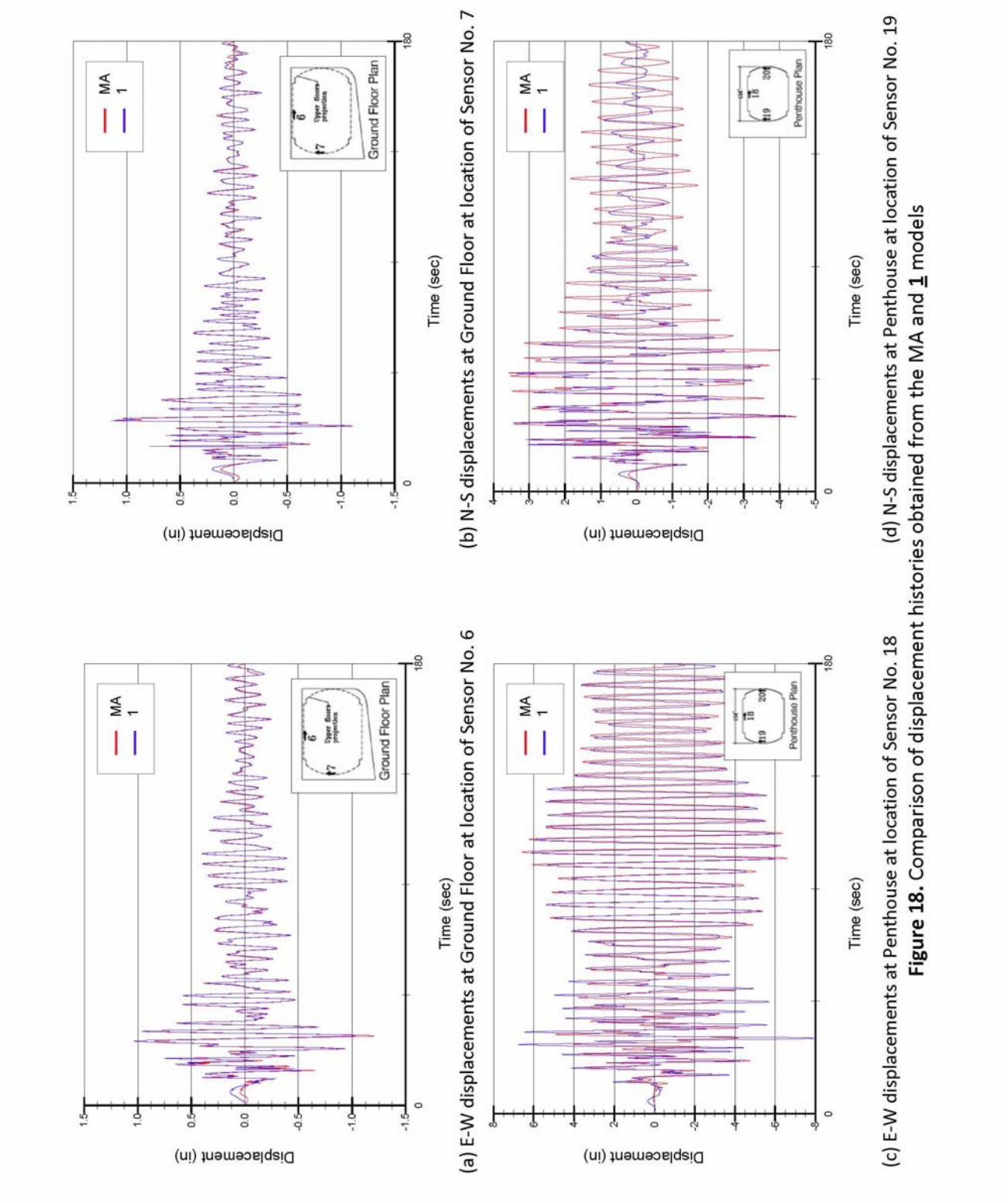

Figure 18. Comparison of displacement histories obtained from the MA and **1** models

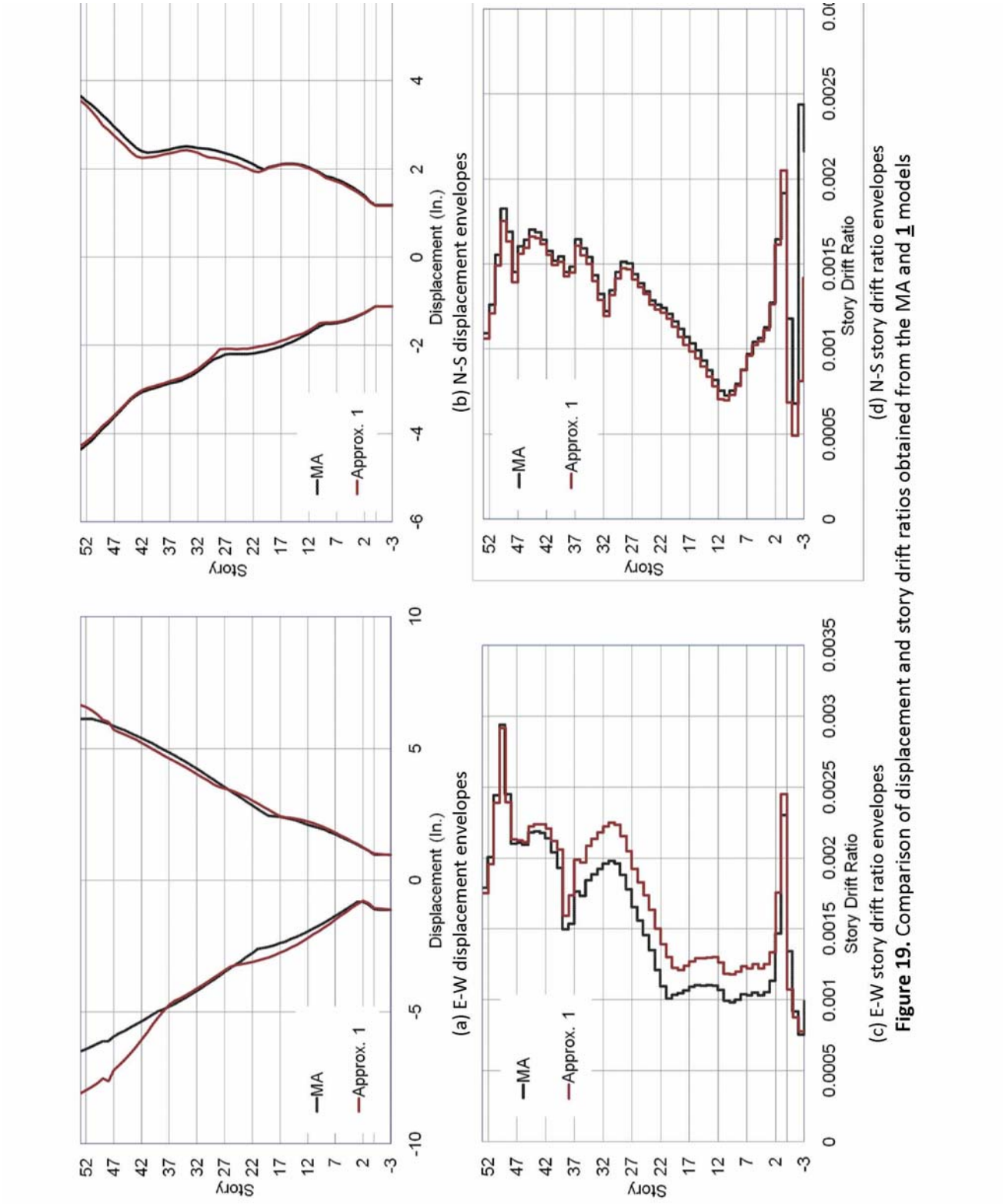

Figure 19. Comparison of displacement and story drift ratios obtained from the MA and **1** models

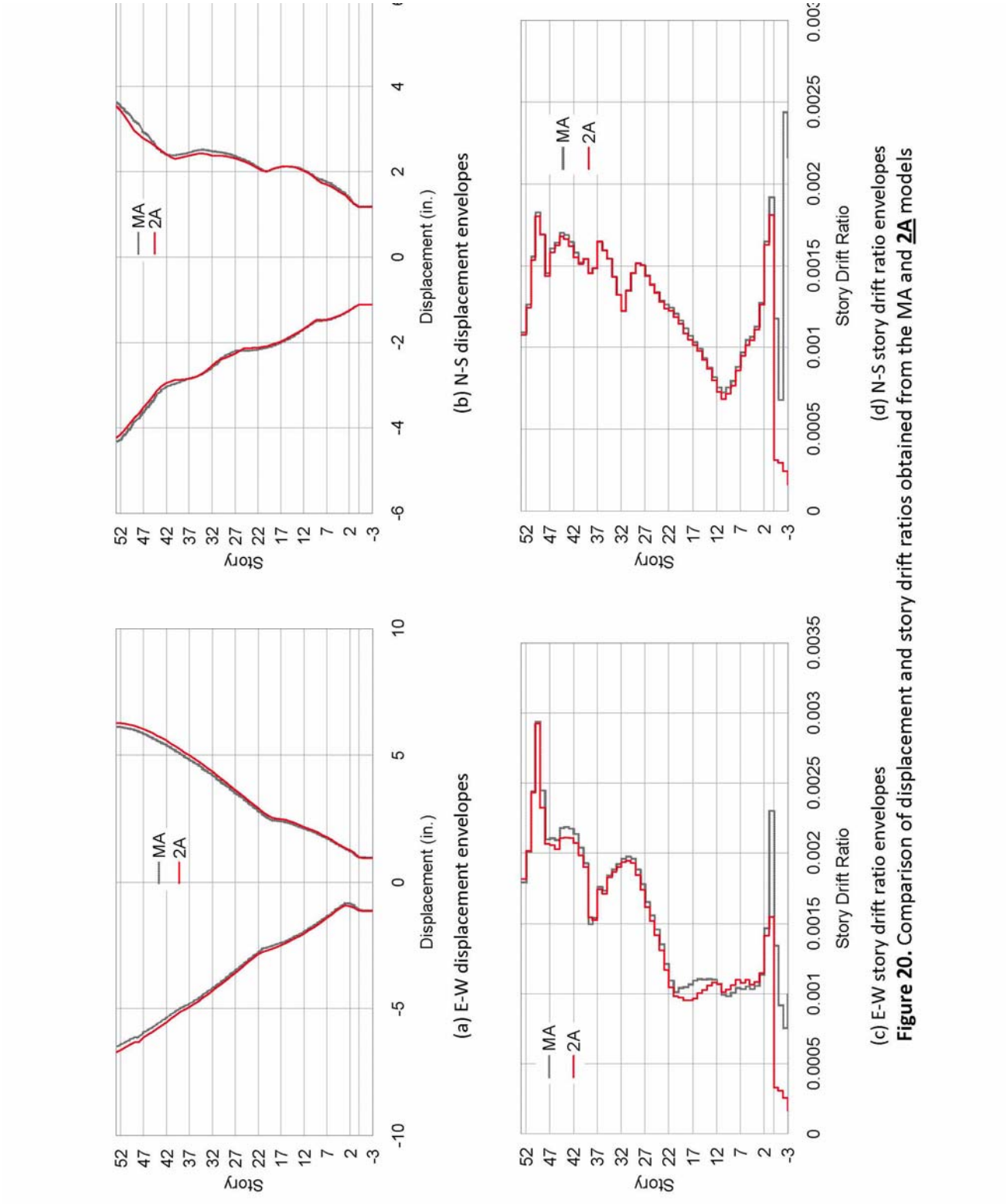

Figure 20. Comparison of displacement and story drift ratios obtained from the MA and **2A** models

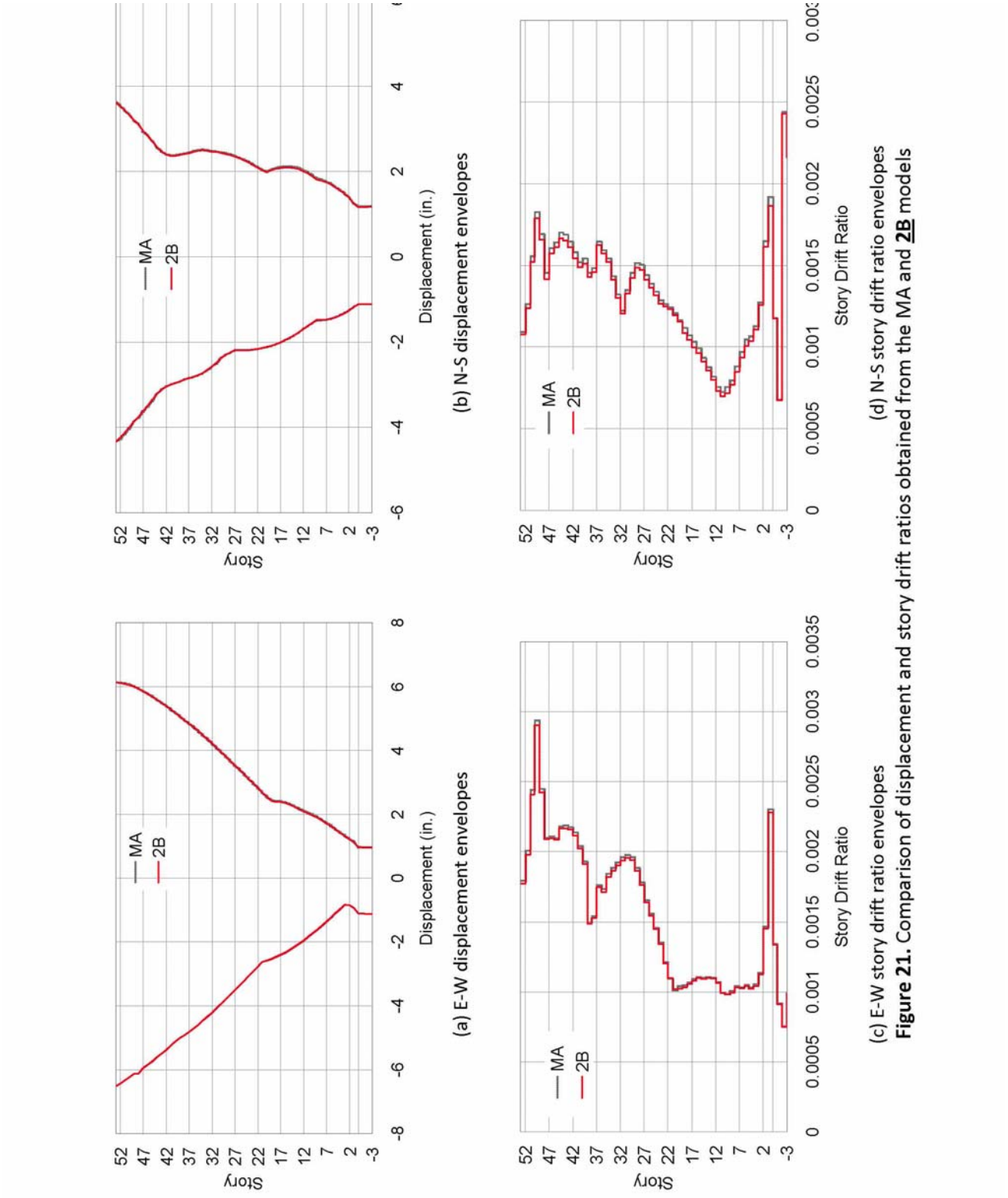

Figure 21. Comparison of displacement and story drift ratios obtained from the MA and **2B** models

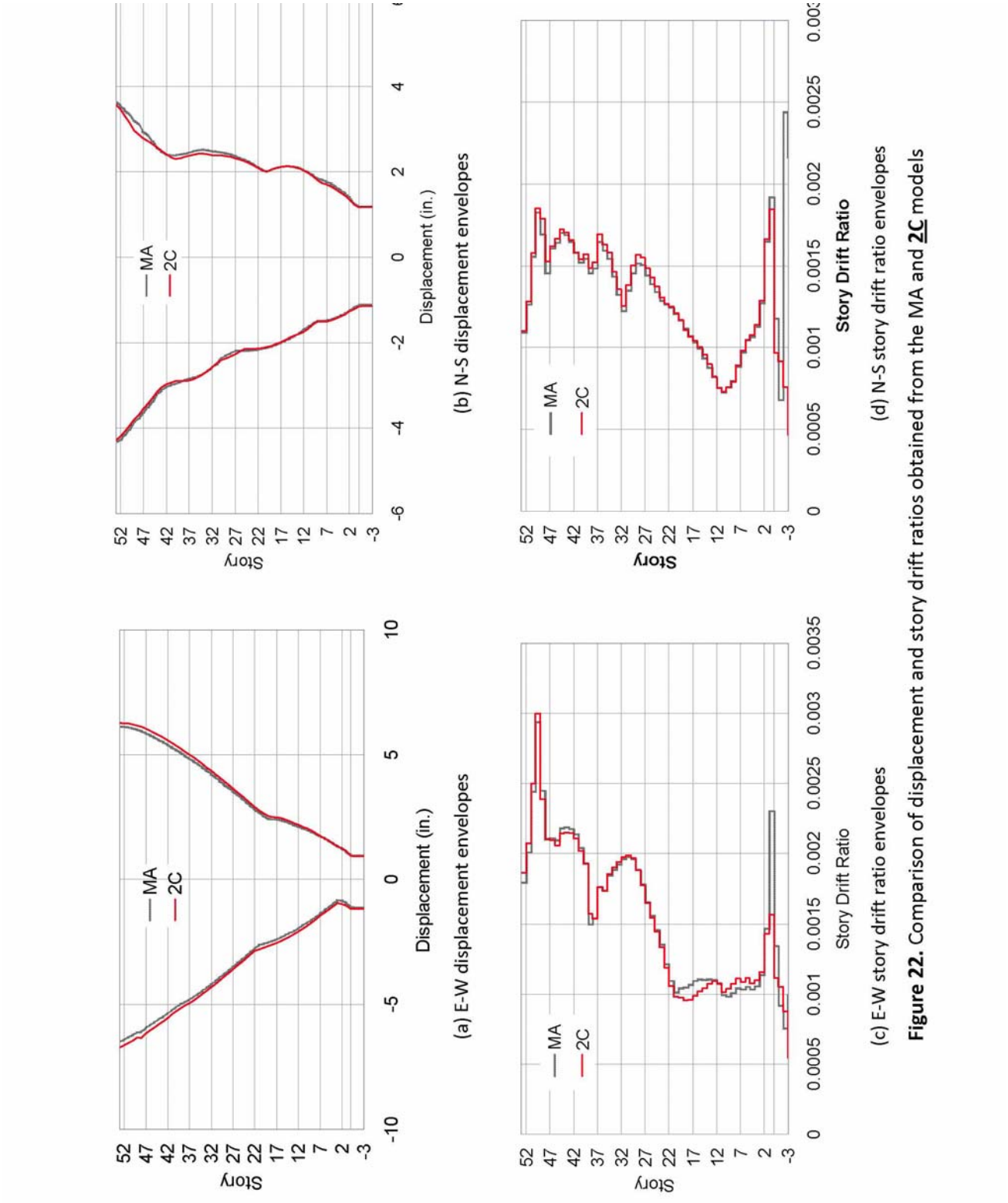

Figure 22. Comparison of displacement and story drift ratios obtained from the MA and 2C models

7.0 Summary and Conclusions

Soil-structure interaction can affect the response of buildings with subterranean levels by modifying the characteristics of input motions relative to those in the free-field and through the added system compliance associated with relative foundation/free-field translation and rocking. While procedures are available to account for these effects, they are seldom utilized in engineering practice. Our objective is to examine the importance of these effects on the seismic response of a 54 story building with four subterranean levels. We first generate a "most accurate" (MA) model that accounts for kinematic interaction effects on input motions, depth-variable ground motions along basement walls, compliant structural foundation elements, and soil flexibility and damping associated with translational and rocking foundation deformation modes.

With reasonable tuning of superstructure damping, the MA model accurately reproduces the observed response to the 1994 Northridge earthquake. While the MA modeling exercise was ultimately successful, the process highlighted several major hurdles to the implementation of soil-structure interaction effects in practice for these types of structures. The principal implementation problems are lack of a direct integration scheme in ETABS and existence of nonphysical acceleration spikes in the acceleration results. These could be rather easily solved by code developers and we are told that such corrections are forthcoming in the near future.

We remove selected components of the MA model one-by-one to test their impact on building response. Factors found to generally have a modest effect on building response above ground level include compliance of structural foundation elements, kinematic interaction effects (on translation or rocking), and depth-variable ground motions applied to the ends of horizontal soil springs/dashpots. However, those factors did generally affect below-ground response as measured by interstory drift.

Properly accounting for foundation/soil deformations does not significantly affect vibration periods for this tall building (which is expected), but does impact significantly the distribution of inter-story drifts over the height of the structure. To our knowledge, the latter observation is new to this study.

Two approximations commonly used in practice are shown to provide poor results: (1) fixing the structure at ground line with input consisting of free-field translation and (2) fixing the structure at the base level, applying free-field motions as input at the base level, and using horizontal foundation springs along basement walls with their end condition fixed to the free-field ground motion.

References

Chajes, M. J. Finch, W. W., Jr., and Kirby, J. T. (1996). "Dynamic analysis of a ten-story reinforced concrete building using a continuum model," *Computers & Structures*, 58 (3), 487-498.

Computers and Structures, 2008, *ETABS version 9 User Manuals*, Berkeley, CA.

EPRI, Electrical Power Research Institute (1993). "Guidelines for determining design basis ground motions. Volume 1: Method and guidelines for estimating earthquake ground motion in eastern North America," *Rpt. No. EPRI TR-102293*, Palo Alto, CA.

Idriss, I.M. and Sun, J.I. (1992). "SHAKE91: A computer program for conducting equivalent linear seismic response analyses of horizontally layered soil deposits," Center for Geotech. Modeling, Univ. of California, Davis.

Kim, S. and Stewart, J.P. (2003). "Kinematic soil-structure interaction from strong motion recordings," *J. Geotech.. & Geoenv. Engrg.*, ASCE, 129 (4), 323-335.

Kunnath, S. K., Nghiem, Q., and El-Tawil, S. (2004). "Modeling and Response Prediction in Performance-Based Seismic Evaluation: Case Studies of Instrumented Steel Moment-Frame Buildings," *Earthquake Spectra*. 20 (3), 883-915.

LeRoy Crandall Associates, LCA (1981). "Report of Geotechnical Investigation, Proposed High Rise Development, Bounded by Harbor Freeway and 7th, 8th, and Figueroa Street, Los Angeles, California," *Job. No. ADE-81040.*

Liu, H., Yang, Z., and Gaulke, M. S. (2005). "Structural identification and finite element modeling of a 14-story office building using recorded data," *Engineering Structures*, 27 (3), 463-473.

Mylonakis, G., Gazetas, G., Nikolaou S., and Chauncey, A. (2002). "Development of Analysis and Design Procedures for Spread Footings" Technical Rpt MCEER-02-0003, City University of New York and the University of Buffalo, State University of New York, 246 pgs.

Naeim, F., Lee, H, Hagie, S., Bhatia,H. And Skliros, K. (2005), *CSMIP-3DV Technical Manual*, John A. Martin & Associates, Inc, Los Angeles, CA.

Naeim, F., Lee, H, Hagie, S., Bhatia,H., Alimoradi,A. and Miranda, E. (2006), "Three-dimensional analysis, real-time visualization, and automated post-earthquake damage assessment of buildings," *The Structural Design of Tall and Special Buildings*, 15, 1, pp. 105-138, Wiley InterScience, London.

PEER, 2008, Open system for earthquake engineering simulation (OpenSees) – development platform by the Pacific Earthquake Engineering Research Center (PEER). *http://opensees.berkeley.edu/.*

Seed, H.B. and Idriss, I. M. (1970). "Soil moduli and damping factors for dynamic response analyses," *Report EERC 70-10*, Earthquake Engineering Research Center, University of California, Berkeley.

Stewart, J.P. and Stewart, A.F. (1997). "Analysis of soil-structure interaction effects on building response from earthquake strong motion recordings at 58 sites," *Rpt. No. UCB/EERC-97/01*, Earthquake Engineering Research Center, University of California, Berkeley, February, 742 pgs.

Stewart, J.P. and Tileylioglu, S. (2007). "Input ground motions for tall buildings with subterranean levels," *Structural Design of Tall and Special Buildings*, 16(5), 543-557.